ELSEVIER

Journal of Marine Systems 33–34 (2002) 63–89

JOURNAL OF MARINE SYSTEMS

www.elsevier.com/locate/jmarsys

# Major changes in Mediterranean Sea level variability from 7 years of TOPEX/Poseidon and ERS-1/2 data

G. Larnicol[a,*], N. Ayoub[b], P.Y. Le Traon[a]

[a]*CLS Space Oceanography Division, 8-10 Rue Hermès, 31526 Ramonville St. Agne, France*
[b]*LEGOS/CNRS, 18, avenue Edouard Belin, 31401 Toulouse Cedex 4, France*

Received 30 January 2001; accepted 29 August 2001

**Abstract**

Seven years of combined maps of TOPEX/Poseidon (T/P) and ERS-1/2 altimeter data are used to describe the surface circulation variability in the Mediterranean Sea. As described in the past, the Mediterranean Sea level variability is a complex combination of a wide range of spatial and temporal scales. However, this paper gives an improved estimation of sea level statistics (rms, annual, semiannual cycle). Moreover, the longer period (1993–1999) and the merging of T/P and ERS-1/2 altimeter data allows us to observe with a good accuracy the major changes that occurred in the Mediterranean Sea and, in particular, at basin and sub-basin scales. First, important interannual signals were found in the Ionian basin where the cyclonic circulation has clearly intensified since 1997. In the Levantine basin, although the Ierapetra eddy exhibits a clear seasonal cycle, it is not always present during our period of observation. These interannual changes seem to be correlated with the variability of the Mid-Mediterranean Jet, which produces strong meanders. A new view of the circulation in the south of the basin is indeed suggested by considering that the eddies observed in the Mersa-Matruh and Shikmona areas represent meanders of the Mid-Mediterranean Jet rather than permanent structures as commonly described. Secondly, the seasonal cycle of the Alboran gyres is confirmed. Moreover, these gyres and the Ierapetra eddy constitute the most intense signals of the Mediterranean Sea variability. Finally, this descriptive study illustrates the need to continue monitoring the surface circulation in order to better understand the dynamics of the Mediterranean Sea. 

*Keywords:* Mediterranean Sea; Altimetry; SST; Interannual and seasonal variability; Eddies

## 1. Introduction

During the last two decades, a considerable amount of work has been dedicated to the study of the Mediterranean circulation. International observation programs in the Western (e.g. WMCE: Western Mediterranean Circulation Experiment, La Violette, 1990) and Eastern (e.g. POEM: Physical Oceanography of the Eastern Mediterranean, Malanotte-Rizzoli and Robinson, 1989) basins, numerous regional in situ data analyses (e.g. in the Liguro-Provençal and Algerian currents, (Millot, 1999), and in the Eastern basin, the recent campaigns described in Horton et al. (1994), together with modeling studies (Tziperman and Malanotte-Rizzoli, 1991; Roussenov et al., 1995; Zavatarelli and Mellor, 1995; Horton et al., 1997 among others) have helped in the early 1990s to identify several structures of the 3D circulation at basin and

* Corresponding author. Tel.: +33-5-61-39-47-53; fax: +33-5-61-39-47-53.

*E-mail address:* glarnicol@pop.cls.fr (G. Larnicol).

0924-7963/02/$ - see front matter 
PII: S0924-7963(02)00053-2

sub-basin scales. If the fate of the Atlantic water from the Gibraltar Strait to its transformation in the Levantine basin in salty intermediate waters and the formation of the so-called Mediterranean Dense Water are relatively well understood, the 'details' of the surface circulation and its variability are still poorly documented and explained. For most of the observed medium-scale (O (100 km)) signals, it is not yet possible to determine whether they are the signature (1) of permanent sub-basin-scale features, (2) of the seasonal or interannual variability of large-scale currents or (3) of sporadic events. The main difficulty in interpreting observations or General Circulation Model (GCM) results is thus the uncoupling between the various spatial and temporal scales.

In this context, remote sensing data, like sea surface temperature (SST), altimetry and ocean colour, have been a very precious tool to obtain synoptic views of the circulation. Sea surface temperature data from satellite infrared imagery have been widely used to follow the Algerian Current instabilities (Millot, 1985). Larnicol et al. (1995) first showed the potential use of TOPEX/Poseidon (T/P) data to monitor and describe the mean sea level and large-scale circulation variability. Vasquez-Cuervo et al. (1996) use ERS-1 altimetric data together with SST observations to study the Alboran gyres, while Ayoub et al. (1998) show that T/P data need to be combined with ERS-1 measurements for the analysis of the sub-basin-scale variability. Mesoscale activity is explored by Iudicone et al. (1998) from a statistical analysis of T/P data. Using Advanced Very High Resolution Radiometer (AVHRR) SST data and buoy trajectories, Matteoda and Glenn (1996) provide a very comprehensive description of the small-scale variability in the Eastern basin over the period 1990–1995. The analysis of satellite data emphasises the large range of the spatial and temporal scales characterising the Mediterranean surface circulation variability. A few authors, including Horton et al. (1994) and Larnicol et al. (1995), show that it is not easy to retrieve from observations over the last 10 years the various structures described in papers relating to POEM data. We point out here the ambiguity linked to the fact that many structures observed during the POEM cruises have been named and thus implicitly identified as well-defined permanent or recurrent features, whereas the very large variability revealed recently by surface observations suggests that the notion of 'permanent' and 'recurrent' structures is questionable.

The work of Matteoda and Glenn (1996) partly addresses this issue. These authors analyse more than 4 years of SST satellite data in the Eastern Mediterranean and identify as persistent features five main eddies: the Ierapetra eddy southeast of Crete, the Pelops eddy south of Peloponnese, a cyclone southwest of Crete, and the Shikmona and West Cyprus eddies in the Levantine basin, all of them named according to previous in situ data analyses (mainly from POEM). Additional eddies are detected but, because they appear only once over the observation period and do not persist for more than a month, the authors consider them as transient features. Besides, the five main eddies mentioned above are shown to display a significant variability in shape and can appear as multi-centered structures. The same observational evidence from combined T/P and ERS-1/2 sea level anomaly data led Ayoub (1997) to use the term 'complex' rather than 'well-defined' structure to describe the variability that is observed recurrently in the Mersa-Matruh, Shikmona or Pelops areas.

The objective of this paper is to explore further the *permanent*, *recurrent* or *transient* character of the main structures of the Mediterranean surface variability. By *permanent*, we mean a variability signal detected over most of the observation period and that has been mentioned in earlier data analyses. We define as *recurrent* a structure that appears on a regular basis even though a period of occurrence may not be possible to define. *Transient* is used to describe an eddy that can be identified for a limited and relatively short period of time only (no more than a few months). Our study relies on the analysis of 10-day T/P and ERS-1/2 altimetric data together with weekly SST maps from October 1992 to December 1999. Since the mean sea level cannot be separated from the geoid surface (see Section 2.1), we use sea level anomaly data with respect to a 4-year mean sea level. As shown later, SST maps help to interpret some features seen from altimetry when the analysis from sea level anomaly instead of absolute dynamic height makes it too ambiguous. On the other hand, altimetric observations contain the signal of subsurface structures that do not necessarily have a surface signature; in other words, some intensified subsurface structures can be detected from altimetry and not from SST observations. However, our study is exploiting further the 7 years of available altimetric data by investigating the possible signs of interannual variability at the basin scale. We focus on the Ionian and Levantine basins, where previous studies have suggested significant changes of the circulation during the last decade (Roether et al., 1996; Ayoub, 1997; Theocharis et al., 1999).

This paper provides a comprehensive description of the major surface variability structures observed from a 7-year altimetric data set. Some hypotheses or suggestions concerning the Mediterranean circulation are proposed with respect to current knowledge. However, we do not attempt to explain the observed variability. We believe that the use of estimation techniques to achieve a model/data synthesis would be the most appropriate tool to provide clues towards a full understanding of the observed signals. The article is divided into six sections. Section 2 describes the data processing and gives details on the T/P and ERS data combination method. In Section 3, we describe the variability from statistics on the SLA, putting the emphasis on the interannual variability. Sections 4 and 5 detail the main structures of the variability evidenced in Section 3: in the Western basin (Section 4) and the mesoscale and sub-basin-scale variability in the Levantine (Section 5.1) and Ionian (Section 5.2) basins. Finally, a conclusion is drawn in the last section.

## 2. Data processing

### *2.1. Data processing (corrections along the track)*

A little more than 7 years of the latest TOPEX/Poseidon (T/P) M-GDRs (Geophysical Data Records) distributed by AVISO (1996) and the ERS-1 and ERS-2 Ocean Products Records (OPRs) distributed by the French Processing and Archiving Facility (PAF) CERSAT (Centre ERS d'Archivage et de Traitement, 1996) are used. They span the period from October 1992 to December 1999; however, ERS-1 data are not available between January 1994 and March 1995 during the period of the satellite geodetic mission. For both data sets, the usual geophysical corrections have been applied (wet and dry tropospheric, ionospheric, electromagnetic, tides, inverse barometer; for details, see Le Traon and Ogor, 1998).

First, merging multiple altimeters requires homogeneous and intercalibrated SSH data sets. Intercalibrated data sets are obtained by performing a global crossover adjustment of the ERS-1/2 orbit, using the more precise T/P data as a reference (Le Traon and Ogor, 1998). The data are then resampled every 7 km along the tracks using cubic splines. In order to eliminate geoid signals, Sea Level Anomalies (SLA) are constructed by removing a 4-year mean (1993–1996) from surface heights. To reduce measurement noise, the SLA are filtered with a 35-km median filter and a Lanczos filter with a cut-off wavelength of 42 km. Finally, the data are subsampled one point in two.

### *2.2. Objective analysis (map construction)*

SLA maps combining T/P and ERS-1/2 data (their respective spatial coverage is shown in Fig. 1) are produced every 10 days on a regular $0.2 \times 0.2^\circ$ grid by using a suboptimal space/time objective analysis (Bretherton et al., 1976). The merging of T/P and ERS data is not trivial. Indeed, despite the intercalibration of the data sets (see previous section), along-track biases due to residual orbit errors and to atmospheric pressure effects (Le Traon and Gauzelin, 1997; Ayoub et al., 1998) remain in both data sets. We apply an improved mapping method based on multi-satellites altimeter data developed by Le Traon et al. (1998). Its principle is to directly take into account the along-track long wavelength error by modifying the a priori error covariance prescribed in the objective analysis method.

More specifically, our analysis is performed using space (isotropic) and time correlation functions with 150-km and 15-day correlation radius. These values are consistent with the along-track correlation scales, estimated by Ayoub et al. (1998) to lie between 80 and 100 km in space and 10 and 20 days (for T/P) in time. The correlation radius are chosen considering the space/time sampling scales of T/P and ERS-1/2 and the need to build an isotropic estimation of the SLA field (i.e. with a homogeneous mapping error field). For more details, the reader is referred to Ayoub (1997). Measurement noise is set to 2 cm rms for T/P and 3 cm rms for ERS-1/2; large wavelength errors are set to 3 cm rms for T/P and 4 cm rms for ERS-1/2 (note that the adjustment of ERS-1/2 SSH data on T/P reduces the long wavelength error level).

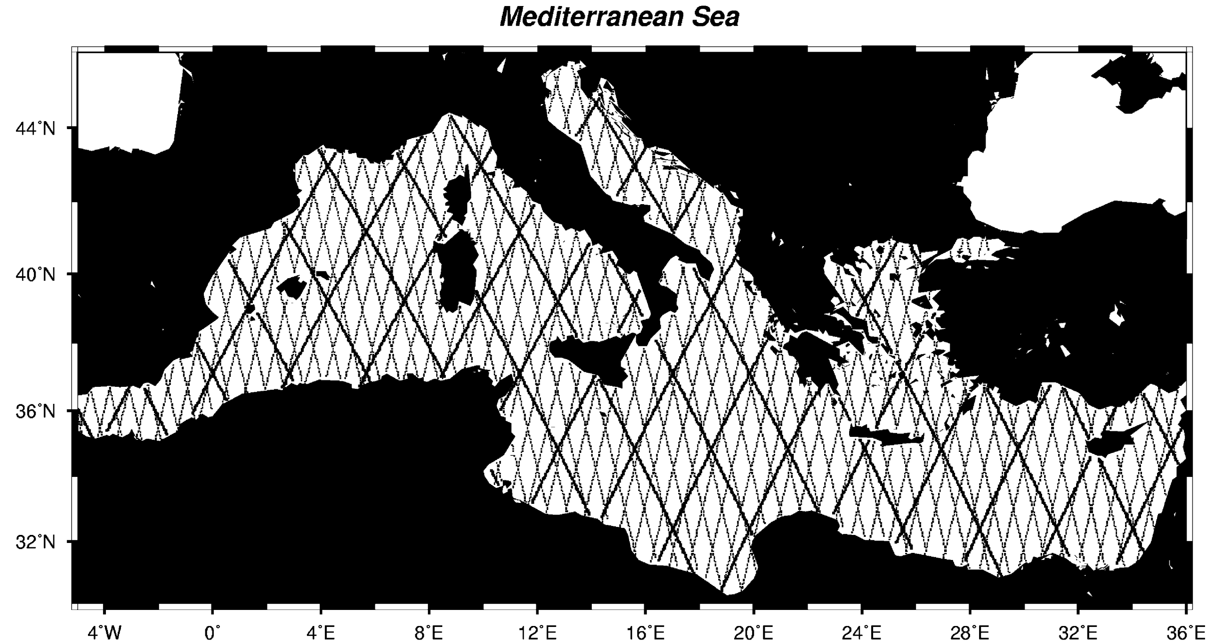


Fig. 1. Spatial coverage of T/P (bold) and ERS-1/2 (dot) altimetric data.

Data interpolation in the Mediterranean Sea presents some complications due to the complicated geometry of the coastline and to the islands. In applying the objective analysis scheme, we have taken care, for example, of using no data from the Tyrrhenian Sea when interpolating in the Ionian Sea and vice versa. Some methods, such as the variational scheme used by Brankart and Brasseur (1998) to interpolate hydrographic fields, are dealing with different statistics in the coastal areas from those in the open sea. Because the satellites sampling properties are uniform over the basin, the use of uniform statistics is justified by the need to maintain a homogeneous mapping error level. Moreover, the analysis of coastal regions where a few altimetric data are available is beyond the scope of this paper.

### *2.3. Sea surface temperature processing*

The sea surface temperature (SST) influences and is influenced by the ocean circulation and the air/sea exchanges at the surface. At small scales, SST measurements can provide information on the mesoscale ocean flow field. Consequently, SST data are potentially useful to confirm whether the specific mesoscale features observed in altimetric data occur or not. SST on a $1/4 \times 1/4°$ grid derived from NASA Pathfinder AVHRR SST daily products are used for this study. The maps are constructed using a median filter applied on the 1/4° grid selecting all temperature values closer than 18 km (two 9-km pixels in the original images) to the estimation point. The median value is preferred to the mean value in order to avoid the influence of data points polluted by clouds. This yields daily maps with a resolution of 1/4°. A time average is then computed every 10 days taking 11 days of data ($d-5$ days, $d+5$ days). Even if there is only 1 day free of clouds for a selected grid point over the whole 11-day period, the average is computed. The available SST maps span the period October 1992–December 1997.

## 3. Overview of the surface variability

### *3.1. Statistical results*

The 7 years of T/P and ERS-1/2 altimeter data (from 1993 to 1999) allow us to update (Fig. 2) the previous map of rms of SLA given by Larnicol et al.

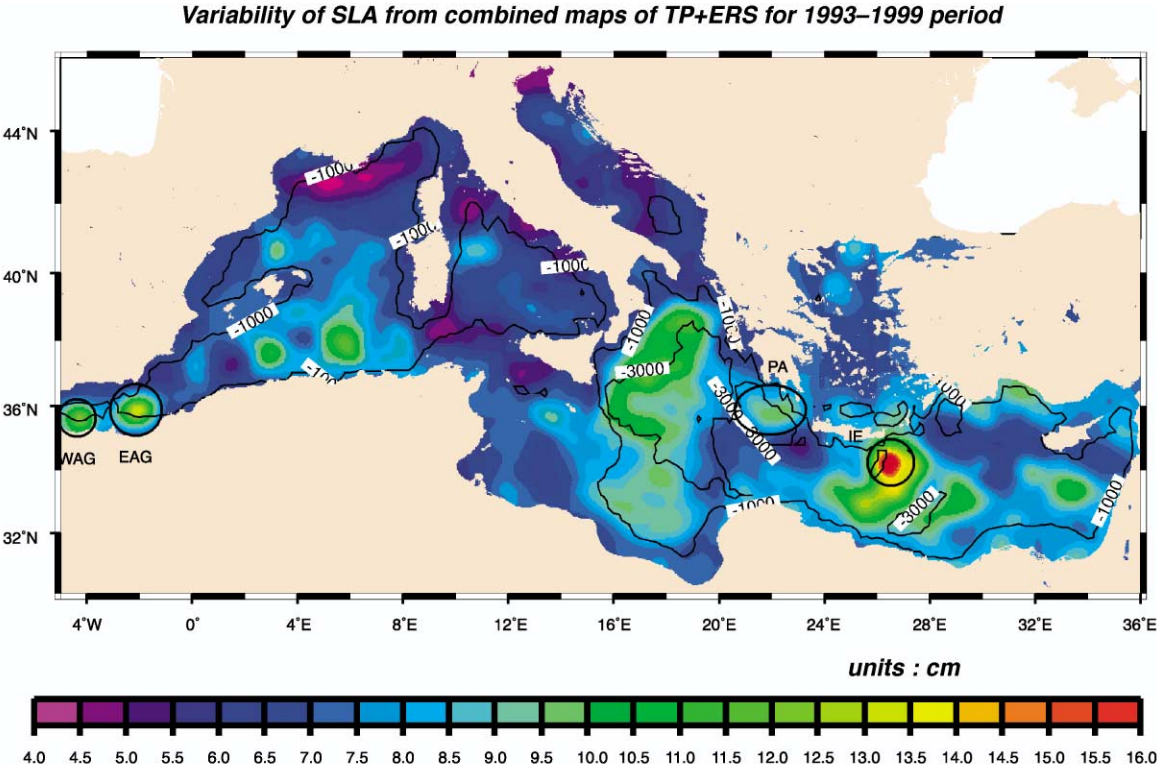


Fig. 2. The rms of Sea Level Anomaly (SLA) deduced from combined maps of T/P and ERS-1/2 for the 1993–1999 period. Units are in cm (the contours correspond to depths of 1000 and 3000 m). WAG and EAG: Western and Eastern Alboran Gyres; PE: Pelops anticyclone, IE: Ierapetra Eddy.

(1995) or Iudicone et al. (1998). Despite the relatively good agreement, these maps are not directly comparable for several reasons. Firstly, they do not represent the same period, and some differences may be induced by interannual variability. Secondly, the present map of rms (Fig. 2) uses ERS data in addition to T/P data. Ayoub et al. (1998) have already shown that combining the two data sets is crucial to yield more information on the circulation variability, and especially on the mesoscale activity. For instance, the variability seen by T/P data only (Larnicol et al., 1995; Iudicone et al., 1998) is preferentially located along the T/P tracks, whereas the areas between T/P tracks are generally characterised by low rms values. These discontinuities in the shape of the rms disappear when we use ERS data, confirming that the combination of the two data sets leads to a better monitoring of the mesoscale variability than with T/P data alone.

A first view of the Mediterranean oceanic surface variability can be given by the rms of SLA over the whole Mediterranean Sea (Fig. 2). Rms values generally range from 4 to 16 cm with a mean value of about 7–8 cm rms. Half of this variability is assumed to be induced by the steric effect, which represents the dilatation/contraction of the water column driven by heat exchanges at the ocean–atmosphere interface (Larnicol et al., 1995; Ayoub, 1997). The other part of the variability concerns the surface circulation that exhibits a large spectrum of spatial and temporal scales. Low patterns of variability ($<5$ cm) are located in the north of the Western basin, along the Liguro-Provençal coast. The regions of intense variability ($>10$ cm) generally correspond with regions of high mesoscale activity, as in the Alboran Sea, Algerian Current or in the Levantine basin where the rms is the strongest of the Mediterranean Sea (up to 16 cm). Although Fig. 2

represents a classical picture, it is the first time that the shape and the intensity of the spatial structures of the variability in the Mediterranean Sea are represented so well. First, this estimation is more robust than that done in previous studies (Larnicol et al., 1995; Iudicone et al., 1998), due to the long time series used for the calculation, which implies 252 maps with a $0.2 \times 0.2°$ resolution spanning over 7 years. Second, merging T/P and ERS-1/2 data considerably increases the spatial and temporal sampling of the available observations of the Mediterranean circulation.

### 3.1.1. Interannual variability of rms

Moreover, this long period allows us to observe the evolution of the Mediterranean variability year by year (Fig. 3). Only two areas are characterised by relatively stable structures. The first one is the region of the Gulf of Lion, where a patch of low variability (2–4 cm rms ) is observed along the coast continuously from 1993 to 1999. The other stable place is the Alboran Sea, where two cells of high variability (>10 cm rms ) are seen throughout the 1993–1999 period. Elsewhere, significant changes in shape and intensity occur. For instance, the changes of the variability patterns in the Levantine basin during the 1993 to 1999 period lead us to define three periods. During the first one (1993–1994), the variability is only characterised by a well-defined signal, up to 16 cm rms, located close to the southeast corner of Crete and referred to as the Ierapetra eddy (Theocharis et al., 1993; Larnicol et al., 1995). From 1995 to 1998, the location of the maximum SLA variability moves to the east (in 1995) then to the southwest (in 1996–1997). In 1998, we can observe two maxima. In 1999, the maximum located near Crete is found again, with low variability in the Rhodes gyre area. A complete description of the variability in the Levantine basin is given in Section 5.1. The situation in the Ionian basin is specific with a strong variability at the basin scale between 1993–1996 and 1997–1999 (see Section 5.2). In 1993, the rms value is around 6–9 cm rms and gradually reaches 16 cm rms over the entire basin in 1999. These strong interannual changes are described in detail in Section 5.2.

## 3.2. Annual cycle

The annual cycle (Fig. 4) is estimated using the 10-day combined maps of T/P and ERS-1/2. Its amplitude (Fig. 4a) is relatively homogeneous in the basin, with values between 8 and 10 cm. A large part of this signal can be attributed to the steric effect (Larnicol et al., 1995) with a maximum sea level in summer. Our analysis suggests a slight lag between the two basins (Fig. 4b, phase), with a maximum occurring in September in the Eastern basin, and in August in the Western basin.

The steric effect is one of the dominant signals on the surface elevation in the Mediterranean Sea. On the other hand, this basin-scale signal does not generate significant geostrophic currents. So, in order to observe dynamic signals, a spatial mean has been removed from each of the 10-day maps. This partly removes the steric effect and puts in a prominent position dynamic signals such as mesoscale activity. As expected, the annual cycle amplitude (Fig. 4c), generally less/lower than 3 cm, is lower than the amplitude deduced previously. Two main areas are only characterised by a relatively important seasonal signal, the Alboran Sea with a value of about 8–9 cm, and the intense Ierapetra eddy with a value of 10 cm. A complete description of the variability in these areas is given further. As a preliminary conclusion, we can decompose the seasonal signal in the Mediterranean Sea into a basin-scale signal, the steric effect, and, in some restricted regions, the cycle of structures at a permanent position (Alboran gyres and Ierapetra eddy). No significant semiannual signal (not shown) has been found across the Mediterranean basin: the amplitude is systematically lower than 3 cm with values close to zero in the Ionian and Levantine basin (< 1 cm).

The variability of the Mediterranean surface circulation is well sampled by our 10-day maps of T/P and ERS-1/2 data. The rms computation reveals the most important changes that occur in the Mediterranean Sea from 1993 to 1999. Several interesting cases are selected: the circulation in the Western basin and, in particular, of the Alboran gyres that exhibit a clear seasonal signal; the circulation in the Levantine basin, where the transient or permanent character of some structures needs to be clarified; and finally, the Ionian basin, where drastic changes have occurred during the last 7 years. The analysis presented in the next sections is based on monthly and seasonal maps from winter 1992 to winter 1999. This series of maps is too long (84 for the monthly means) to be inserted in the

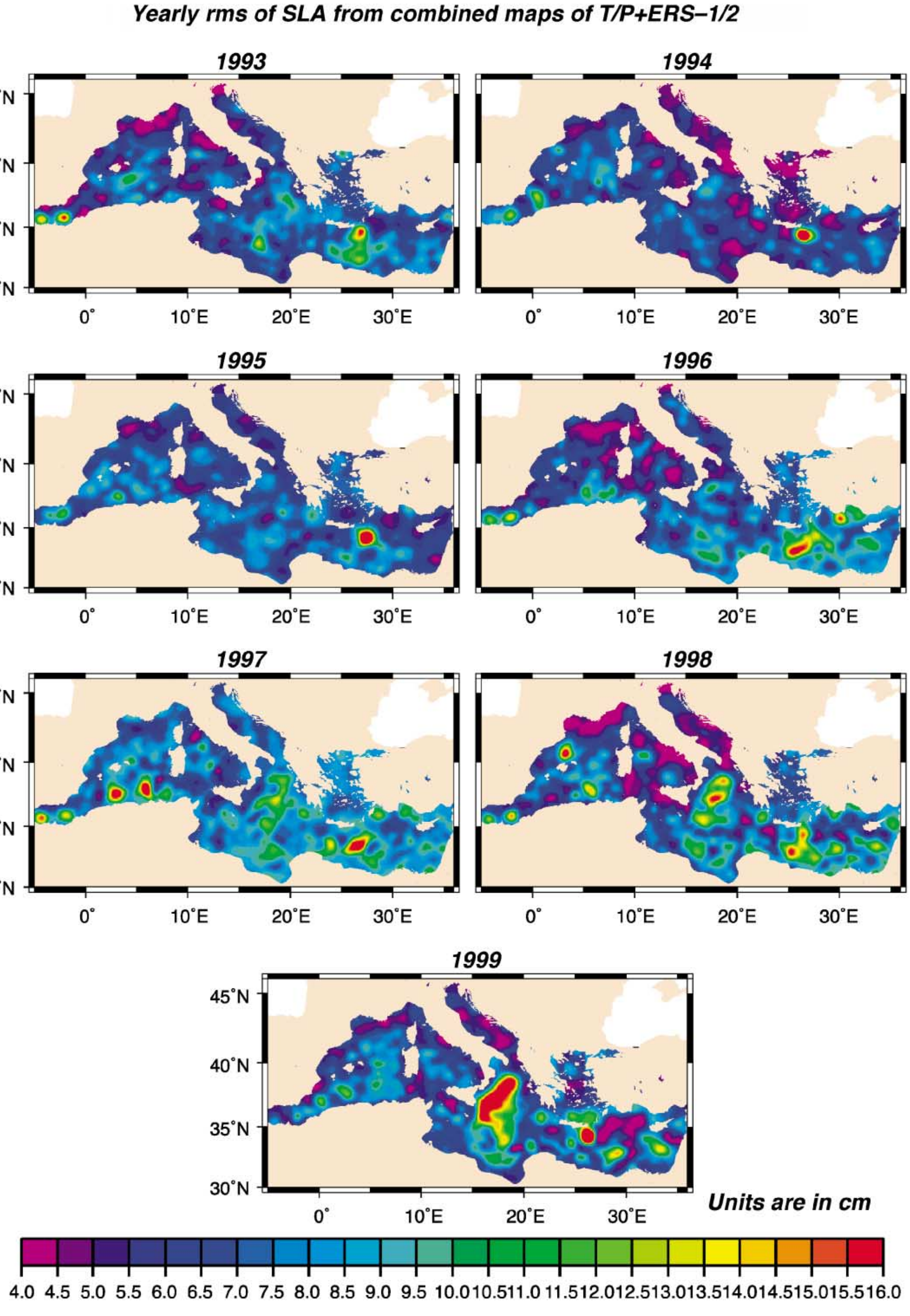


Fig. 3. Yearly rms of Sea Level Anomaly (SLA) deduced from combined maps of T/P and ERS-1/2 between 1993 and 1999. Units are in cm.

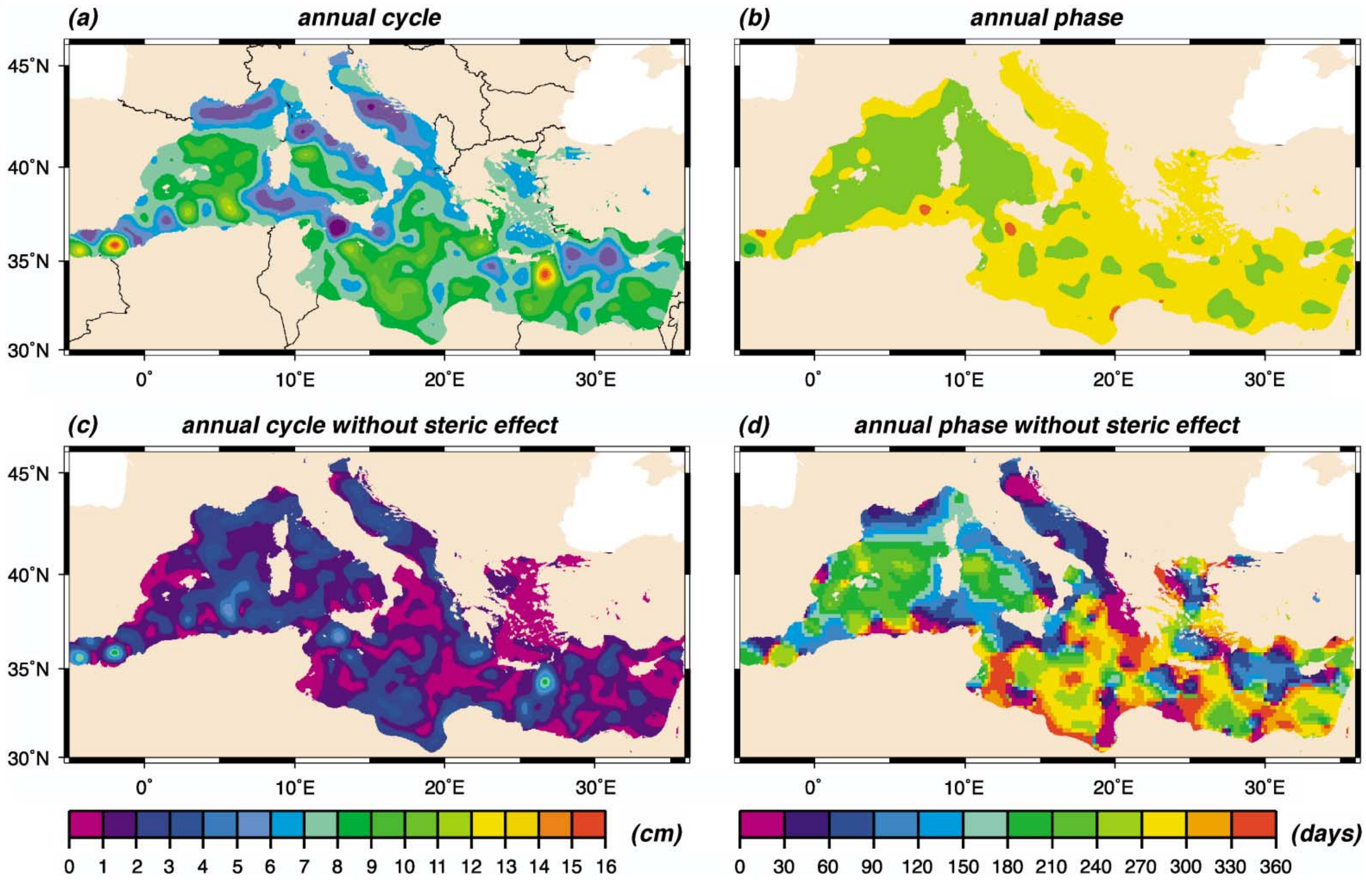


Fig. 4. Annual signal amplitude (a) and phase (b). The annual signal amplitude (c) and phase (d) are deduced from SLA maps from which the spatial mean of each map has been removed. Units are in cm for the amplitude, and in days for the phase.

paper, so only specific maps are shown when necessary.

## 4. Western basin

### 4.1. Algerian Current

After passing through the Gibraltar Strait and the Alboran Sea, the Atlantic water forms the well-known Algerian Current. This unstable current generates meanders of a few tens of kilometers and, simultaneously, a series of coastal cyclonic and anticyclonic eddies characterised by a radius of 50 to 100 km, and a short lifetime. Only the anticyclonic eddies can develop and separate from the current (Millot, 1999). The signature of the Algerian Current and its variability are clearly seen in the rms maps (Fig. 2), with a background value varying between 8 and 10 cm rms. Note that the use of ERS-1/2 altimeter data significantly improves the estimation of this variability.

Moreover, year-by-year analysis of the rms exhibits some interesting interannual changes. In particular, strong changes appear in 1997 where two patches of variability (up to 16 cm rms) are clearly visible along the Algerian coast. They are centered on 3°E/37.5°N and 6°E/38°N with a radius of approximately 150 km. In fact, they correspond to the signature of two anticyclonic Algerian eddies (AE) recently monitored by Puillat et al. (2002) with AVHRR images. The authors describe the trajectory of two AE (96-1 and 97-1) that have a lifetime of about 2–3 years. The first eddy, 96-1, seen for the first time in March 1996, stays a little more than 1 year between 5–8°E and 37–39°N. Then it moves westward towards Ibiza. The second eddy appears in March 1997 at 0.5°E/36.2°N, then it moves eastward until the end of the year, is virtually permanent during the winter, and finally continues its eastward movement until 7°E, where it does a large clockwise loop during 1998 year. These eddies are very well sampled by 10-day maps, and have also a clear signature in monthly and seasonal means. This paper focuses rather on the seasonal and interannual circulation than on mesoscale monitoring. Nevertheless, it seems important to mention the existence of such long-lifetime AEs, which have a strong signature in the spatial and temporal structure of the surface variability seen by altimetry (Fig. 3e). Moreover, the two intense patches of variability correspond to specific characteristics of the eddies' trajectory (quasi-stationary period, small loop). Indeed, the maximum variability exactly corresponds to the location where the eddies stay for a relatively long time (see the trajectory and the rms maps of 1997). That is the reason why we observe two patches of rms greater than 16 cm in 1997, and rms greater than 10 cm between 4°E and 8°E in 1996 and 1998. As a conclusion, we suggest that the classical activity of the Algerian Current, its meanders and the small eddies generate an activity of about 6 to 8 cm rms, whereas rms greater than 10 cm likely correspond the occurrence of long-lifetime AEs.

### 4.2. A Balearic eddy

Another important mesoscale phenomenon was revealed by combined T/P and ERS maps in the Balearic Sea, with the appearance of an intense anticyclone during July 1998 (Fig. 3f, 1998). The anticyclone remains almost stationary, with an SLA amplitude of about 20 cm until the end of February 1999. This anticyclone is seen in both SLA and SST data, as well as in an oceanographic cruises carried out in the region in February 1999 ("Hivern-99"). The presence of the anticyclonic structure produces a significant change in the general circulation of the Balearic basin. The thermohaline structure, the origin and the life of this eddy are discussed in a specific paper (Pascual et al., 2002).

### 4.3. Alboran Sea

The classical circulation of the Alboran Sea, as usually described in the literature, is characterised by a wavelike front coupled with one and eventually two large anticyclonic gyres, the Western and the Eastern one (WAG and EAG), respectively situated at −4.5°E and −2°E (Viudez et al., 1996). The latest studies in this narrow passage show that the variability of the surface circulation of Atlantic water is relatively high (Vasquez-Cuervo et al., 1996; Heburn and La Violette, 1990). This is confirmed by our analysis with rms of SLA greater than 10 cm for the whole area. Fig. 2 clearly exhibits two maxima of variability that correspond to the Alboran gyres activities. The respective values are 13–14 cm rms for EAG and 11–12 cm rms for WAG. Regarding the previous estimations deduced from 2 years of T/P data only (1993–1994) and given by Larnicol et al. (1995) or Iudicone et al. (1998), the intensity and the shape of the variability in our analysis seems to be better described. This is mainly due to the optimal combination of ERS-1/2 and T/P data and to the long time series (7 years). Compared to the work of Ayoub et al. (1998) over the period October 1992 to December 1993, the extension of the observation period to 7 years leads to an improved representation of the gyres' variability.

It is important to recall that the temporal resolution of our maps is not sufficient to discuss the high-frequency variability ( < 10 days) of the Alboran gyres. By construction, the SLA do not allow us to conclude definitively about the presence or disappearance of the Alboran gyres; we discuss here their temporal variations with respect to the 4-year mean sea level. Our analysis concentrates on the seasonal-to-interannual variability of the gyres occurrences as cyclonic (negative) or anticyclonic (positive) signals on SLA maps. Assuming that the gyres location is unchanged over the analysis period, an anticyclonic signal can be interpreted as intensification of the gyres whereas a cyclonic signal indicates a gyres weakening. The WAG and EAG signatures as positive/negative signals are listed in Table 1. They exhibit a relatively clear seasonal cycle, intensifying during summer and weakening during winter. A slight phase lag of 1 or 2 months is observed between WAG and EAG. Indeed, it seems that EAG is maximum between August (1995, 1997) and October (1993, 1996, 1998), whereas WAG is maximum between June (1993, 1995), July (1996, 1998) and August (1996, 1997) periods. The amplitude of this seasonal cycle is about 10 cm (Fig. 4). This description confirms that the seasonal variability in the Alboran Sea is one of the most important signals observed in the Mediterranean Sea. The gyres are particularly well observed in the seasonal means of 1993 (Fig. 5a) and 1998. Moreover, the 10-day maps (not shown) allow us to follow with great accuracy the variations in shape and intensity of both gyres. In this case, the spatial structure of the SLA is in complete agreement with the description given by Viudez et al. (1996) from CTD measurements. For instance, the radius estimated from the 10-day maps is comprised between 80 to 120 km. On the other hand, due to the spatial resolution of altimetric data, the small cyclonic eddies seen by Viudez et al. (1996) on the western side of both gyres are not sampled. To our knowledge, nobody has yet presented such a long time series of data and characterised the long-term variations in this region. This long time series allows us to separate the various temporal frequencies and, in particular, to gain more confidence about the estimated annual signal here with respect to the one discussed in Larnicol et al. (1995) from 2 years of data.

Table 1
Cyclonic (C, SLA < 0) or anticyclonic (A, SLA>0) state of the western (WAG) and eastern (EAG) Alboran gyres from 1993 to 1999, deduced from monthly combined maps of T/P and ERS data

| | | 1 | 2 | 3 | 4 | 5 | 6 | 7 | 8 | 9 | 10 | 11 | 12 |
|---|---|---|---|---|---|---|---|---|---|---|---|---|---|
| 1993 | WAG | **C** | **C** | C | | A | **A** | **A** | A | A | **A** | **C** | |
| | EAG | **C** | **C** | **C** | **C** | **C** | | A | | A | **A** | **C** | |
| 1994 | WAG | C | | C | | | C | | | | | C | |
| | EAG | | **C** | C | C | | A | **A** | A | | | A | A |
| 1995 | WAG | C | C | | | **A** | **A** | | | | | | |
| | EAG | | | | | A | | **A** | | **A** | | | |
| 1996 | WAG | | A | C | C | **A** | **A** | | **A** | **A** | **A** | **A** | A |
| | EAG | | **C** | **C** | **C** | C | C | | A | A | **A** | **A** | A |
| 1997 | WAG | | **C** | **C** | C | **A** | **A** | **A** | **A** | | | | |
| | EAG | A | | | C | **C** | A | **A** | **A** | **A** | | | |
| 1998 | WAG | **C** | **C** | **C** | C | **A** | A | **A** | A | A | | **C** | |
| | EAG | **C** | **C** | **C** | **C** | **C** | A | A | **A** | **A** | **A** | A | |
| 1999 | WAG | C | C | | **A** | A | | | | | | | |
| | EAG | **C** | C | C | | **A** | **A** | | | | | | **C** |

The cyclonic or anticyclonic states are with respect to the 4-year mean and do not represent the absolute states of the gyres. Characters in bold mean that the intensity of the gyre is greater than 10 cm. (Note that due to the lack of ERS data, we used T/P maps from January 1994 to March 1995.)

The analysis of the 10-day maps also highlights extra-seasonal variability. In particular, numerous authors have already shown that the anticyclonic gyres could disappear over a period of a few days (Heburn and La Violette, 1990; Perkins et al., 1990). Recently, Vargas et al. (1999) have revealed a situation with three anticyclonic gyres. They assume that this case is an anomalous situation that mainly occurs during autumn and spring, while in summer, the circulation seems more stable. Obviously, we have observed some disappearances of the Alboran gyres, but no situation similar to the one described in Vargas et al. (1999) is clearly detected in the altimetric maps. The high frequency and the weak spatial extent of such a signal are probably not resolved by the altimetric spatial and temporal sampling. Moreover,

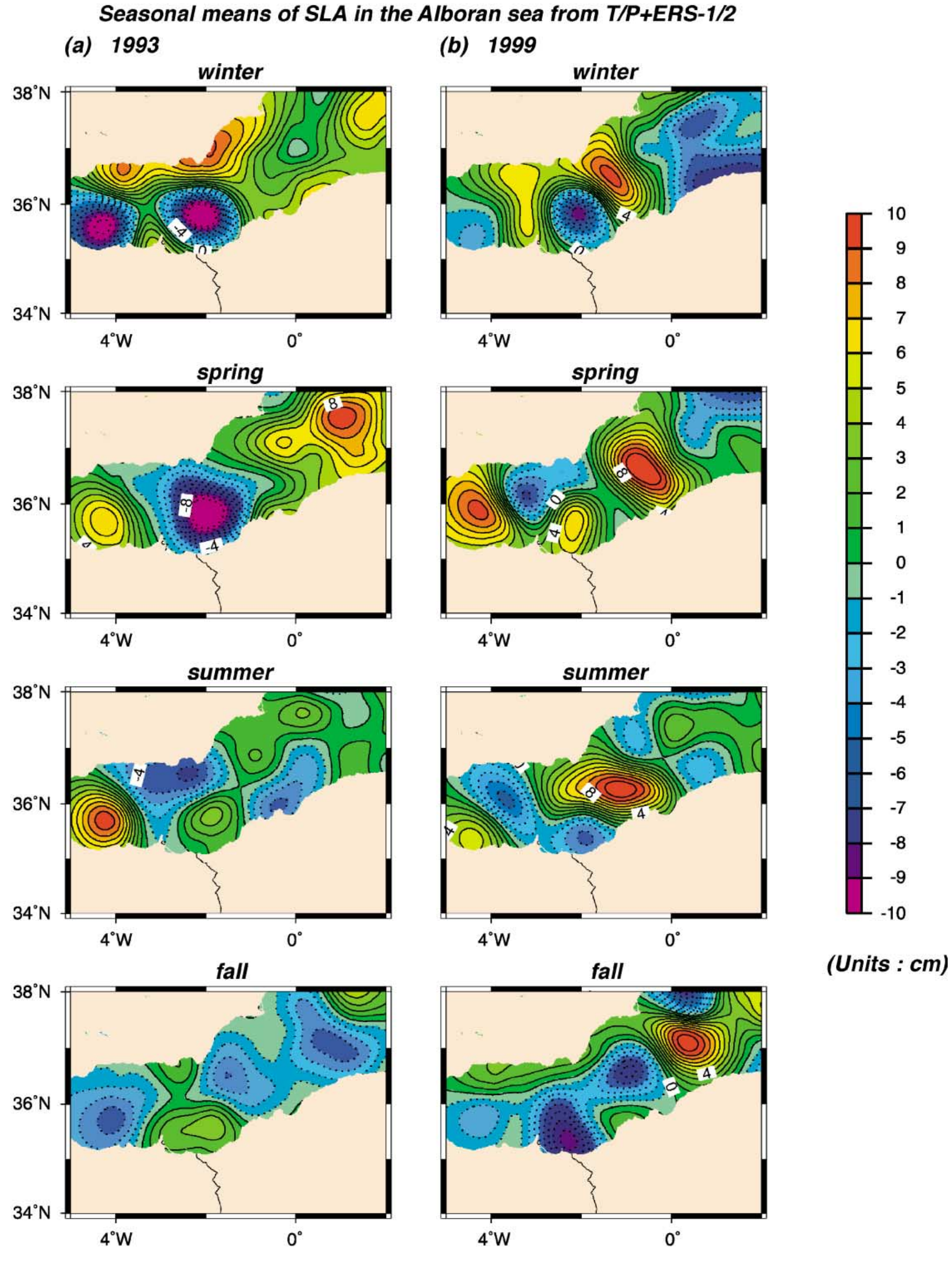


Fig. 5. Seasonal means of SLA in the Alboran Sea in 1993 (a) and in 1999 (b) deduced from combined maps of T/P and ERS-1/2. Units are in cm.

these anomalous situations (disappearance or occurrence of three eddies), if they have a long lifetime, could strongly perturb the seasonal cycle. This could be what we observe in 1999: there is no signature of the gyres' intensification in summer. However, this is the only year that such an anomaly is detected, so we can conclude that the seasonal signal in the Alboran Sea is relatively stable from 1 year to the next during the period 1993–1999. Analysis of the 10-day maps also shows that the appearance/disappearance of the WAG and the EAG are not correlated. The reasons for this variability are not clear, and still remain an open question. Nevertheless, recent numerical models suggest that the variability of the general circulation in the Alboran Sea could be related to the inflow/outflow through the Gibraltar Strait (Speich et al., 1996).

## 5. Eastern basin

During the last 20 years, numerous observational and modeling programs such as POEM have been dedicated to the study of the Eastern Mediterranean Sea. The description given by the POEM group proposes a scheme of the surface circulation with a jet-like zonal current named the Mid-Mediterranean Jet (MMJ), linking the Ionian and the Levantine basins. Around the MMJ, many sub-basin-scale gyres and mesoscale eddies induce an important variability. A major conclusion of the previous studies is the complexity of the circulation due to the strong influence of wind forcing and the orography of the bordering land areas. For most of the observed features of the circulation, their permanent, recurrent or transient character is still an open question. This section especially aims at describing the mesoscale eddies (diameter roughly varying between 150 and 300 km) by analysing altimeter and sea surface temperature data, and consequently to discuss the statements in the literature on the recurrent, permanent or transient properties of these features. Similar analyses were conducted by Horton et al. (1994) with intensive AXBT surveys, and by Matteoda and Glenn (1996) from 4 years of AVHRR data.

### *5.1. The case of the Levantine basin*

The Levantine basin is divided into five regions of high variability: southeast of Crete with the Ierapetra eddy (IE), the Mersa-Matruh and Shikmona areas, east of Cyprus, and south of Turkey. The minimum variability ( < 6 cm rms) is located in the north of the basin, between Crete and Cyprus. It probably corresponds to the region of the Rhodes gyre, which is described in the literature as a permanent feature of the circulation, characterised by a weak variability.

As mentioned in Section 3 (Fig. 2), the basin is characterised by an rms of 9 to 11 cm with a maximum (>16 cm) associated with IE variability. The extraction of the basin-scale annual cycle (Fig. 4) has shown that IE is the only clear seasonal signal in the Levantine basin with an amplitude of about 20 cm (10 cm when the steric effect is removed). Its phase implies a maximum intensity in summer, more precisely in August. IE was not described in detail by the POEM group although it was clearly seen in the MAR89 (Özsoy et al., 1993) and SEP87 (Theocharis et al., 1993) campaigns. Recently, dedicated studies (Horton et al., 1994; Matteoda and Glenn, 1996) have shown that IE is the most prominent feature on AXBT and AVHRR observations. As suggested by Horton et al. (1994), this eddy could be generated by a local wind stress curl created by the interaction of dominant northerly winds in summer (the 'Etesians') with Crete's orography. The resulting anticyclonic eddy (IE), located southeast of Crete, can persist for several months. So far, the hypothesis about IE wind-induced generation has not been confirmed, with, for example, numerical experiments. In particular, there are still open questions about how IE persistence once the Etesians have stopped blowing. The recent work of Horton et al. (1997) suggests other mechanisms: in their simulation, IE intensification and weakening show a good correlation with the flow variations through the Kasos strait.

The long time series of combined maps of T/P and ERS is analysed in terms of observed occurrences of IE as an anticyclonic (+) or cyclonic ( − ) structure in monthly maps. The first 2 years are characterised by a strong anticyclone which is maximum in late summer in 1993 and in summer in 1994 (15 and 35 cm, respectively; Fig. 6a and b). These observations, especially the position of the anticyclone's centre (26.5°E, 34.5°N), are in a perfect agreement with the description of Matteoda and Glenn (1996). Note also that Horton et al. (1997) are able to reproduce IE in 1993 by forcing their model with wind fields which take

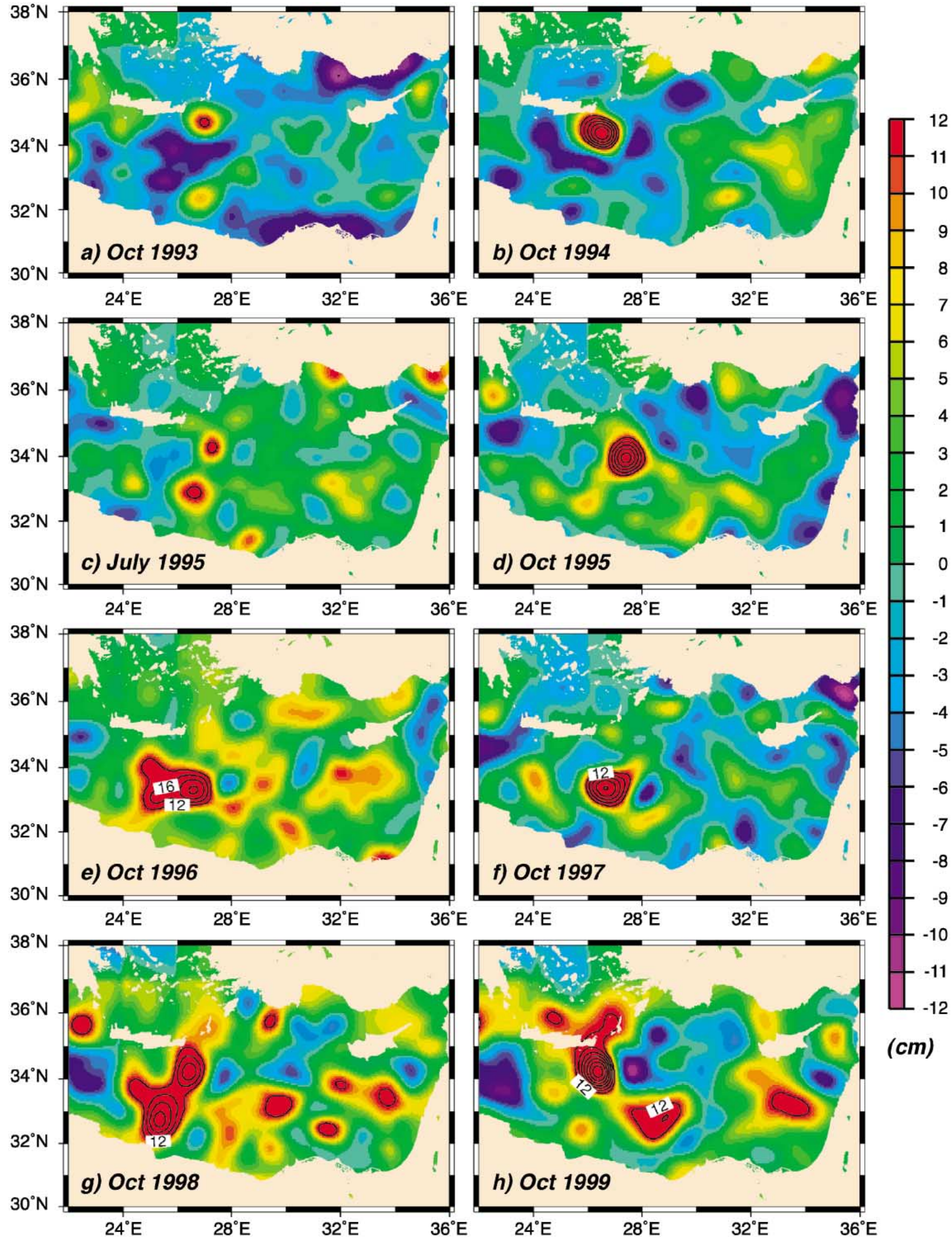


Fig. 6. Monthly means of SLA in the Levantine basin. (a) October 1993; (b) October 1994; (c) July 1995; (d) October 1995; (e) October 1996; (f ) October 1997; (g) October 1998; (h) October 1999. Units are in cm. Contours are drawn every 4 cm (but only for values greater than 10 cm).

into account continental orography. Their success in modeling IE underlines the role played by the wind on the eddy forcing. Nevertheless, it seems that the simulated IE was much weaker than the observations. In 1995, IE appears early in July a little bit further south than in 1993 and 1994. At the same time, we can observe a second anticyclone situated to the southwest of IE (Fig. 6c). This anticyclone can be followed in altimeter maps since May 1995; we believe it does not correspond to IE as suggested by Matteoda and Glenn (1996) (see in Fig. 2 AVHRR images where the location of the eddy seems to be too far from the eastern coast of Crete). From July, IE is continuously growing until the beginning of September 1995, where it seems that the two anticyclones interact. In October 95 (Fig. 6d), they merge into a structure that we still refer to as IE, but located further southeast (27.2°E, 34°N) than in 1993 and 1994. In 1996 and 1997, the situation is completely different with no occurrence of an anticyclone near Crete, but with a large intense anticyclone (up to 25 cm) further south at 33–33.5°N (Fig. 6e and f). The yearly maps of SLA rms (Fig. 3) confirm this description, with maximum intensity located far south of Crete during the 1996–1997 period. Consequently, the patch of variability does not belong to the area between 26–27°E and 34–35°N according to Matteoda and Glenn (1996). Moreover, the 1996–1997 years are characterised by an important variability in the whole basin, probably resulting from the appearance of numerous cells in the SLA. Like 1995, 1998 seems to be a transition year because we can observe strong mesoscale signals in the south (32.7°N, 25°E) simultaneously with the development of IE near the southeast corner of Crete (Fig. 6g). As far as IE is concerned, 1999 seems to be similar to 1993 and 1994 with an intense IE, up to 35 cm in summer (Fig. 6h).

This description of the Levantine basin variability during the 1993–1999 period obtained from altimetric data yields some new ideas about the general circulation in this basin. Unfortunately, due to a not enough accuracy of a mean reference for our SLA data, we cannot state about of IE permanence. Nevertheless, the SLA analysis enables us to identify two distinct states between 1993 and 1999. The first (1993, 1994 and 1999) is characterised by an intense IE adjacent to the eastern corner of Crete, with a significant seasonal variability. During the second period (1996–1997), IE never appears. Instead, large anticyclones develop more to the south between 25–27°E and 32.5–33.5°N. Before the appearance of the large anticyclones, no clear circulation can be established, and the spatial structure of the SLA is composed of multiple cyclonic and anticyclonic cells. We suggest that these cells represent changes of the mean circulation rather than coherent eddy structures. Lastly, 1995 and 1998 are probably transition years.

With the help of SST maps (see Section 3.2), which are very useful to characterise the mesoscale features observed by altimetry, we propose a new interpretation of the variability of the southern Levantine basin. At this point, it is useful to discuss the Levantine basin nomenclature proposed during the last decade. Indeed, we feel that it is not completely satisfactory to name each anticyclone that appears in the Levantine basin Mersa-Matruh or Shikmona. The analysis of all the anticyclones observed from SLA and SST maps shows that the fluctuation in position, shape and intensity is relatively large. This is confirmed by several studies. In particular, Marullo et al. (1999a,b) do not clearly observe the Mersa-Matruh gyre with SST data. Brankart and Brasseur (1998) also note the absence of the Mersa-Matruh gyre in the MODB climatology (The MODB Group, 1996). In this context, defining the Mersa-Matruh and Shikmona gyres as coherent structures like the Alboran or Ierapetra gyres may not be appropriate. They mainly correspond to an area of intense variability which is close to the description of Matteoda and Glenn (1996). The new idea we propose in the article is to no longer describe these anticyclones as coherent structures, like described in Robinson et al. (1991), but instead to associate the occurrence of anticyclones/cyclones in the Mersa-Matruh and Shikmona region with a signature of the MMJ meanders).

Introducing the notion of meanders, Horton's hypothesis can be interpreted as follows: in the absence of IE (1996–1997), the MMJ, which is characterised by a thermal front, flows south of Crete, forming a large loop embedding the anticyclones previously described with the SLA maps and also present in the SST maps (Fig. 7d and e). When IE is fully developed (1993–1994–1999), it constrains the MMJ (Fig. 7a,b,h) to flow and meander more to the south. On the other hand, we can note that during the transition period (1995 and 1998), we still have very

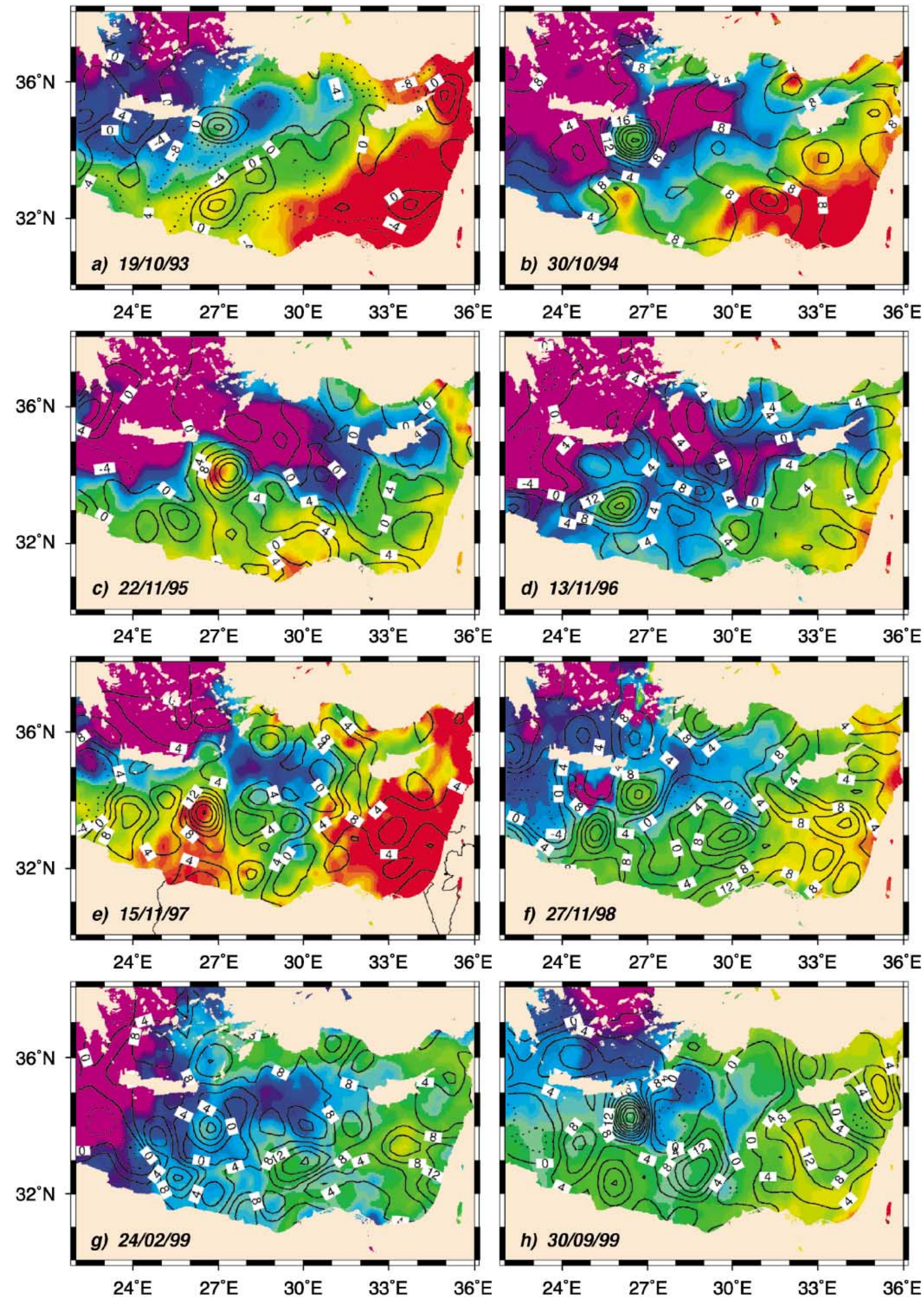


Fig. 7. Comparison between SLA (contours spaced every 4 cm) and SST (colour) in the Levantine basin: (a) 19/10/93; (b) 30/10/94; (c) 22/11/95; (d) 13/11/96; (e) 15/11/97; (f ) 27/11/98; (g) 24/02/99; (h) 30/09/99. N.B.: The SST scale is adapted for each figure to exhibit the most interesting gradient, so it is not indicated in the figure.

consistent signatures of the eddies in the SLA and the SST maps (Fig. 7c and f), which supports our confidence in our observations.

At this step, we can make an slight analogy with the Algerian Current and the MMJ, since both currents meander and tend to generate mesoscale activity. However, one main difference between the MMJ and Algerian Current systems is that our analysis of SST and SLA maps does not reveal any eddy propagation in the Levantine basin like those observed in the Algerian basin (Millot, 1985; Beckers and Nihoul, 1992; Ayoub et al., 1998). Moreover, the analogy has some limitations concerning the mechanisms underlying the meanders and eddies generation. In both the Levantine and Algerian basins, the circulation is expected to be strongly constrained by the topography. For example, the intrusion of a 2000-m deep valley onto the continental shelf coincides with the location of a recurrent anticyclonic activity (referred in the literature as the Shikmona gyre). However, the geometry of the bathymetric contours differs significantly in the two basins and is expected to play different roles in shaping the two currents' paths: in the Algerian Current area, the continental shelf breaks along a steep slope parallel to the coast, whereas in the Levantine basin, shallow (22–25°E and east of ~ 32°E) and deep ( ~ 25–32°E) areas are successively observed off the Libyan and Egyptian coasts (Fig. 2). Moreover, in the case of the Algerian Current, the shear between surface Atlantic water and deep and intermediate Mediterranean waters is assumed to generate baroclinic instabilities (Mortier, 1992). Such a mechanism may occur in the MMJ system, but the Atlantic water in the Levantine basin has likely lost some of its initial properties by mixing with the surrounding Mediterranean water masses on its way toward the Eastern basin. Lastly, atmospheric wind forcing is supposed to play a significant role on the general circulation in the Levantine basin, which in turn could influence the MMJ path and the eddies generation. To our knowledge, atmospheric forcing impact on the Algerian Current system, on the contrary, has never been evidenced.

### 5.2. Ionian basin

The surface circulation in the Ionian Sea is little known, mainly because of the very few in situ data available at the basin scale. POEM data from the March–April 1986 and September–October 1987 cruises (Nittis et al., 1993; Theocharis et al., 1993) led to the identification of some small-scale structures in the northern part of the basin (e.g. the Pelops anticyclone), but to our knowledge, no data-based analysis, other than climatology, is available for the circulation south of ~ 35°N. Numerical simulations over the whole Mediterranean Sea (e.g. Tziperman and Malanotte-Rizzoli, 1991; Roussenov et al., 1995; Zavatarelli and Mellor, 1995) agree on the coarse features of the mean circulation but lack the necessary resolution to solve the variability seen in satellite or in situ data. The classical scheme views the surface flow of Atlantic water as an eastward jet, the Ionian Atlantic Stream (IAS), crossing the basin along either a southern zonal route or a meandering path off Sicily and east of ~ 20°E. In the southern region, analysis of altimetric data (Ayoub et al., 1998) suggests the development of an intense mesoscale activity.

#### 5.2.1. Basin-scale circulation

The inverse modeling study of Tziperman and Malanotte-Rizzoli (1991) and the simulation of Pinardi and Navarra (1993), forced by monthly climatological mean winds, suggest that the Ionian basin-scale circulation undergoes a significant seasonal variability. This latter consists mainly in a shift of the IAS to the north in summer and an intensification of the jet along its southern zonal path in winter, resulting in a cyclonic circulation in the north of the basin. The POEM data analysis of Nittis et al. (1993) tends to confirm the presence of a large anticyclonic meander off the coast of Sicily in the late summer of 1987. SST observations indicate a strong seasonal cycle as illustrated in Fig. 8 for the year 1999. In winter, we observe a well-marked front between the warm water masses associated to the IAS south of ~ 35°N and the colder ones in the north. In summer, the temperature field is characterised by homogeneous and relatively warm values in the central basin, while colder water masses are found east of ~ 20°E. The eastern front follows a northwest–southeast axis north of 36°N, and shows a quasi-meridional orientation south of Peloponnese. However, its location varies slightly from year to year (Fig. 9). Marullo et al. (1999a) interpret this front as the signature of the

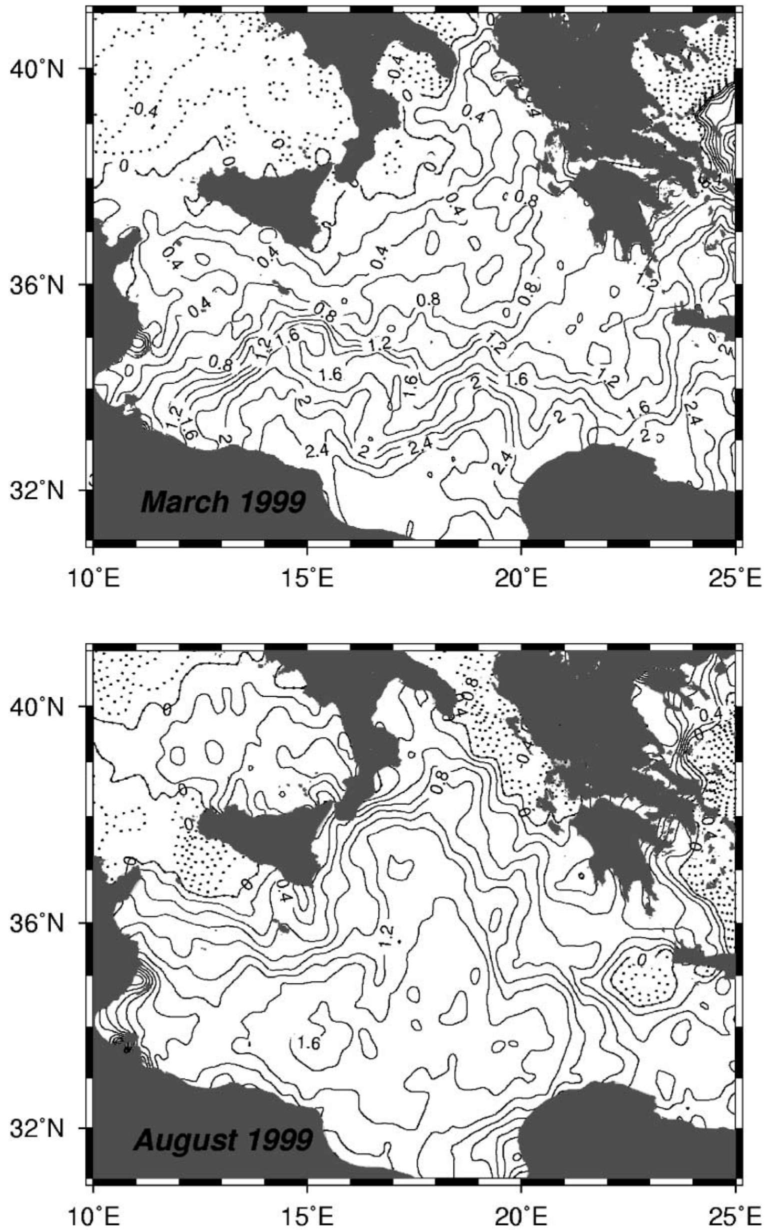


Fig. 8. Monthly means of SST for March and August 1999. The mean over the Ionian basin is subtracted at every grid point on each map. Units are in °C (isocontour: 0.2 °C).

anticyclonic meander formed by the IAS during summer. The shifts between the summer and winter modes occur very regularly over the 1993–1999 period: the 'summer mode' appears roughly in mid-May, the 'winter mode' roughly in late September. The presence of a seasonal cycle in SST variability is quite obvious if we consider that SST is mainly forced by local atmospheric heat fluxes. However, it con-

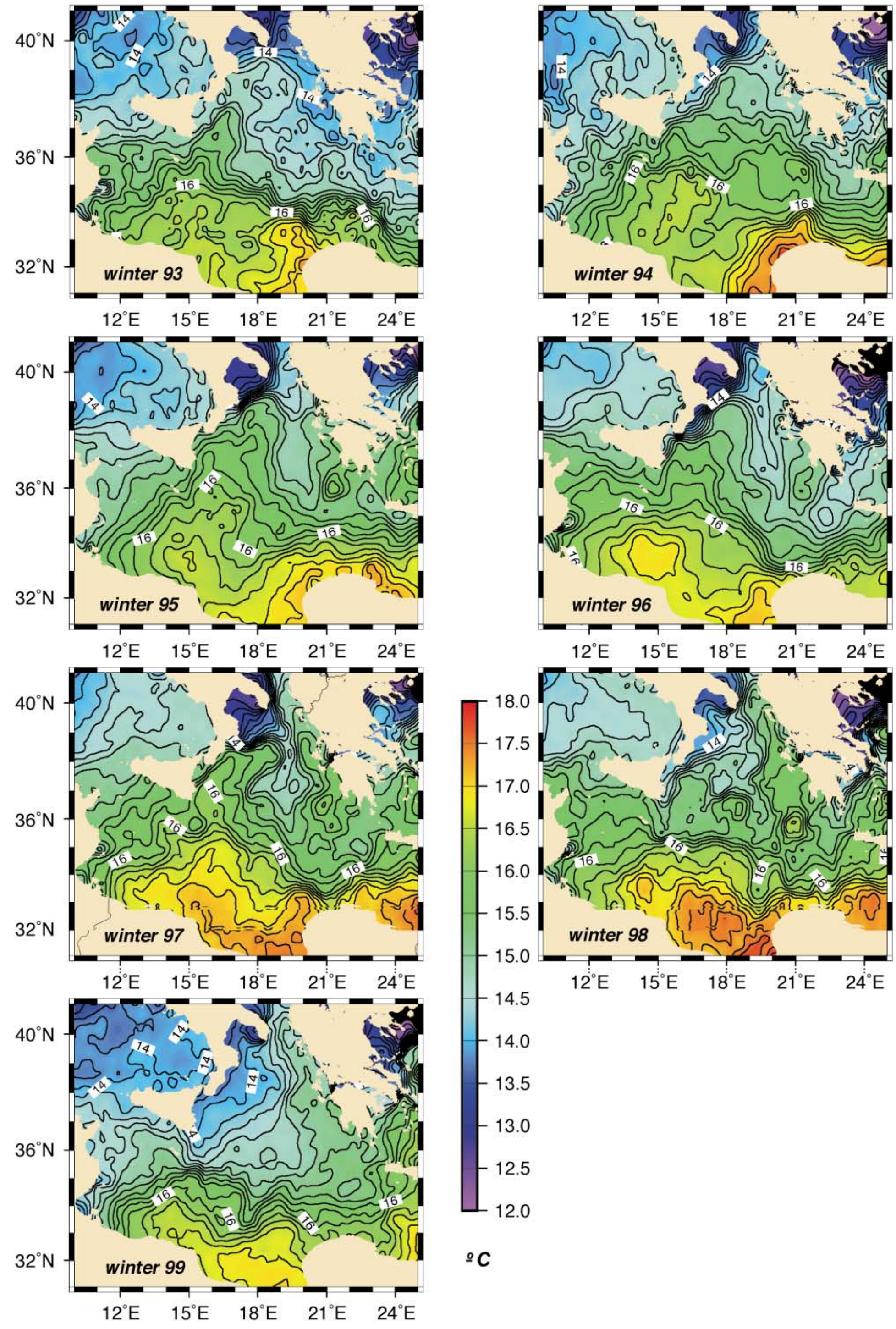


Fig. 9. Seasonal winter means of the SST in the Ionian basin from 1993 to 1999. Units are in °C.

firms the southern path of the IAS in winter during the whole period of study; moreover, it allows us to 'date' the transition from one season to the other.

The maps of SLA seasonal averages (Fig. 10) suggest large-scale seasonal variations consisting mainly in a cyclonic basin-scale circulation (with respect to the mean) in winter and spring and an anticyclonic circulation from June. The presence of small-scale signals, superimposed to the basin-scale circulation and attributed to eddies or IAS meanders (see below), makes impossible an estimate the magnitude of this annual cycle. The simulation of Horton et al. (1997) shows consistent results with our observations. By assimilating XBT and CTD data in a high-resolution model, they show that the main pattern during summer 1993 is a large anticyclone in the northwestern area of the Ionian basin. In winter 1994, the simulation indicates an intense eastward current along the African coast. In the altimetric maps of Fig. 10, the eastward acceleration is suggested by a cyclonic signal in the central part of the basin.

A change of the basin-scale circulation occurs in 1997 when a cyclonic gyre located in the northwestern part of the basin is maintained throughout the year. From January 1998, the gyre spreads and intensifies. It then persists in the north and center of the basin until December 1999. The zone of maximal slope bordering the cyclone to the south extends almost zonally at $\sim 34-35\,^{\circ}$N and seems to follow the bathymetric contours marking the break of the Tunisian continental shelf east of 15 °E. The cyclone undergoes seasonal variations with an intensification in late winter and spring. South of 35 °N, small-scale anticyclonic structures are depicted throughout both years. Fig. 11 shows the mean SLA over the period January 1997–December 1999. Since the SLA are constructed by removing the mean SSH over January 1993–December 1996, the map of Fig. 11 indicates the difference of the mean surface circulation between these two periods. It suggests that the cyclonic signal observed on the maps of Fig. 10 and the increase of variability over 1997–1999 as revealed by Fig. 3 are the signature of a drastic change of the mean circulation in 1997–1999 with respect to the prevailing circulation in 1993–1996. Wintertime SST observations tend to confirm this interpretation: as shown in Fig. 9, the north–south SST gradient west of $\sim 20\,^{\circ}$E is steeper in 1998–1999 than in the previous years. The appearance of a strong cold anomaly is consistent with the presence of the cyclonic circulation. Note also that the persistence of a cyclone in the northwestern part of the basin throughout the year is in good agreement with the simulations of Roussenov et al. (1995). Fig. 11 also highlights an asymmetry between the events occurring in the Ionian and Levantine basins. While the cyclonic circulation in the northern Ionian basin is strengthened, intense mesoscale anticyclonic structures develop in the Levantine (see Section 5.1). This parallelism favours the hypothesis of large-scale interannual variability affecting the whole Eastern Mediterranean circulation. In particular, the renewal of deep and intermediate water masses in the Eastern basin, as discussed by Klein et al. (1999) from January to February 1995 in situ measurements, is likely to have a signature on sea surface heights through density variations. Moreover, the changes in water masses distribution affect the exchanges at the straits in the Cretan Sea (e.g. Kasos Strait) which, in turn, could have some impact on the circulation in the northern Levantine. Horton et al. (1997) show, for example, that the Ierapetra eddy variability is linked to the flow variations at the Kasos Strait. Therefore, one can assume that the changes as described by Klein et al. (1999) have a direct impact on the surface circulation in the Levantine since 1995 (see in Section 5.1 about IE variability) through flows at the Cretan Arc straits for instance, whereas the influence on the Ionian thermohaline circulation (as detected by altimetry) is felt more recently. Local atmospheric forcing can also be responsible for the surface circulation change since 1997. Numerical simulations (e.g. Pinardi and Navarra, 1993) suggest that the seasonal variability is induced by wind stress curl seasonal cycle. A similar mechanism at interannual time scale is possible.

### 5.2.2. Southern region

South of 35 °N, the circulation is characterised by the development of small-scale anticyclonic structures. Some of them are observed over several months. This is the case, for example, of an eddy at about 17 °E/34 °N from June to December 1993 (also described in Ayoub et al., 1998) and of two eddies at $\sim 18\,^{\circ}$E/33 °N and 17 °E/35 °N respectively, from April to November 1997. We do not depict any evidence of seasonal enhancement of the mesoscale activity.

Some of the anticyclones show westward propagation at about 33°N. The attempts so far to define the propagation characteristics (phase speed) have not allowed us to conclude on the nature of these signals, in terms of waves, for example. The propagations are observed on relatively short distances and east of ~ 15°E only. Most of the anticyclones seem 'trapped' by the bottom topography, namely at the sharp break of the Tunisian continental shelf along a quasi-meridional line (at ~ 15/17°E), as represented by the 1000- and 3000-m bathymetric contours in Fig. 2. In the simulations of Tziperman and Malanotte-Rizzoli, an anticyclone is modeled at ~ 17°E/33°N in summer and fall and is interpreted as a recirculation of the IAS. We are indeed tempted to consider the observed anticyclonic eddies as meanders or instabilities generated by the IAS, as suggested earlier for the Levantine basin. However, the only evidence in in situ data of such structures is reported by Nittis et al. (1993). These authors analyse three anticyclones between 35°N and 37°N, embedded in the anticyclonic basin-scale flow, and show that different water masses form the eddies' cores (one of them is a vertical plume of Atlantic water). They deduce that the eddies are of distinct origins, which obviously invalidates the assumption that the eddies are formed instabilities of the IAS.

### 5.2.3. The Pelops anticyclone

The Pelops anticyclone has been described as one of the dominant structures revealed by the dynamic height fields estimated from POEM data (Nittis et al., 1993; Theocharis et al., 1993). The data analysis of late winter 1986 (Theocharis et al., 1993) evidences the Pelops anticyclone as a double-centered gyre. The centers are located south of the Peloponnese (22–23°E, 36°N) and along the western Greek coast (21–22°E, 37°N). In September–October 1987, a single center is observed at the surface at about 21–22°E and 36°N, whereas two of them are revealed at subsurface level by the analysis of Nittis et al. (1993). Using AVHRR SST observations, Matteoda and Glenn (1996) identify the anticyclone as a warm-core eddy. They suggest it is a persistent feature of the Ionian circulation, although the eddy's occurrence is subject to interannual variability. For example, it is observed continuously from October 1990 to April 1992, then disappears and is not detected anymore, except briefly in early 1994 and at the end of the observation period (early 1995). The eddy's location and shape display also some variability. Matteoda and Glenn (1996) show that the eddy can move westward of their suggested mean position at around 36°N and 21°E, with an excursion of 230 km.

To take into account this spatial variability in the analysis of the 10-day SST and SLA maps, we identify as the signature of the Pelops anticyclone (PA) any warm/anticyclonic eddy located in an area roughly included between 20–23°E and 35–37°N. Over the whole observational period, PA appears either as a single eddy or as a structure with two or even three (in 1999) centers. In their simulation, Horton et al. (1997) note the intermittent formation of one or a few anticyclones south and southwest of Peloponnese. We distinguish three main locations for the single eddy or for one of the centers, corresponding to the locations found in the literature, that is: south of the Peloponnese (22–23°E, 36°N), along its western coast (21–22°E, 37°N), and to its southwest at about 21–22°E and 36°N. Fig. 12 illustrates these three different cases. Table 2 summarizes the observed occurrences of PA (with no distinction between the three locations). The time variability of the Pelops anticyclone is complex. There are some long periods where no anticyclonic signals can be detected in the Pelops area, mainly during the spring and summer of 1995 to 1997. Because the indetermination of the mean sea surface makes it impossible to draw a definite conclusion about the persistence of the eddy, we base our analysis on the assumption that the mean sea surface in the Pelops area is flat. An anticyclonic signal therefore indicates the appearance of PA whereas a null or slightly negative SLA means its disappearance.

It would be long and tedious to describe precisely the occurrences of PA at its different locations, so we just summarize our findings. The observations suggest that an eddy appears in fall–winter south of the Peloponnese. In winter, there is generally a second center off the western Greek coast. In 1994, 1998 and

Fig. 10. Seasonal means of SLA in the Mediterranean Sea from 1993 to 1999: (a) winter (January–February–March); (b) summer (June–July–August) The mean is subtracted at every SLA grid point, on each map. Units are in cm.

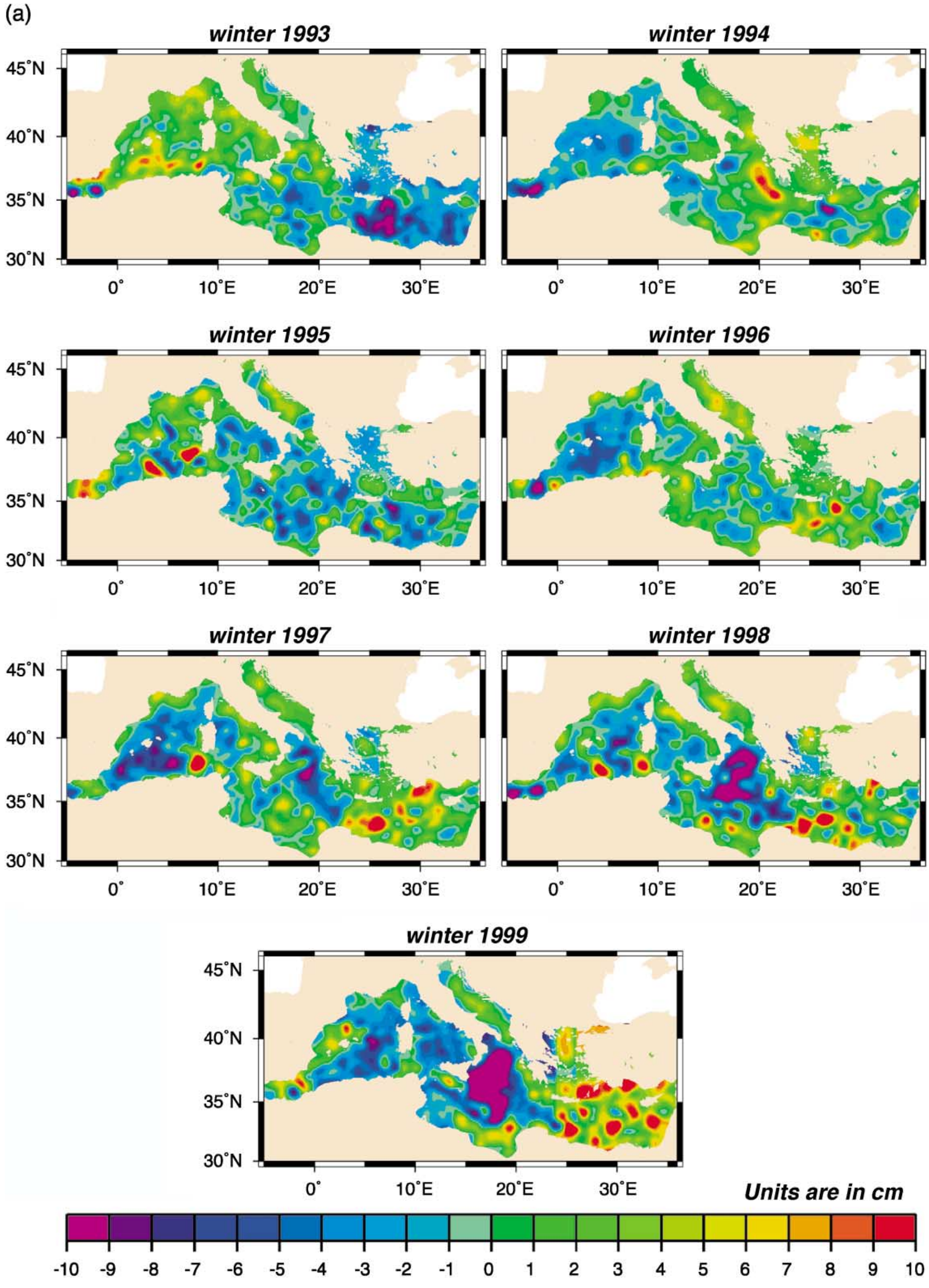
(a)
winter 1993
winter 1994
winter 1995
winter 1996
winter 1997
winter 1998
winter 1999
45°N
40°N
35°N
30°N
0°
10°E
20°E
30°E
Units are in cm
-10
-9
-8
-7
-6
-5
-4
-3
-2
-1
0
1
2
3
4
5
6
7
8
9
10

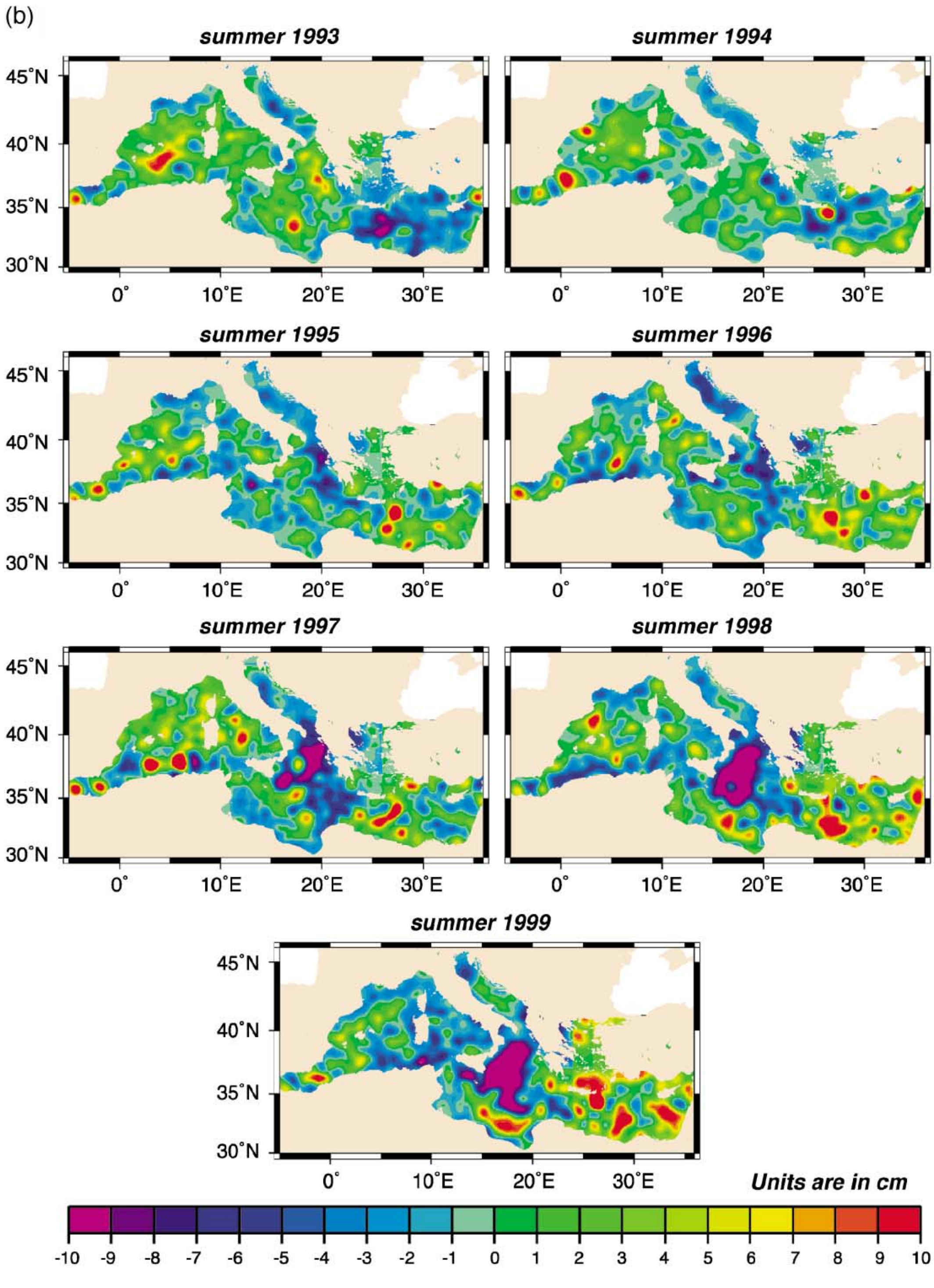


Fig. 10 (*continued*).

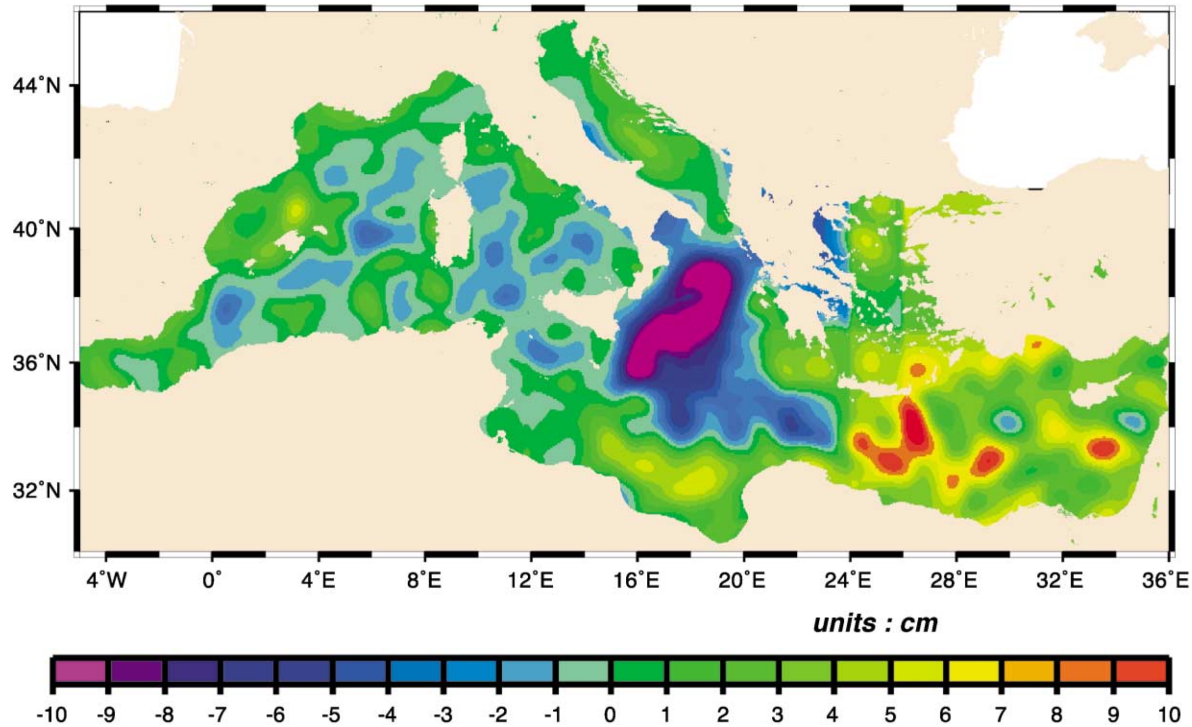


Fig. 11. Mean sea surface for the period 1997 to 1999 computed from the 10-day maps of TP and ERS-2. Units are in cm.

1999, the eddy initially located south of the Peloponnese seems to move westward toward the center of the Ionian basin (at about 21–22°E and 36°N), where it remains during the spring–summer period. The years 1993 and 1999 are special cases in that PA is observed throughout the year. In 1993, it has a very strong signature off the western Peloponnese coast, already described in Larnicol et al. (1995) and Ayoub et al. (1998). In 1999, the persistent feature is mainly an eddy located at ~ 36°N between 21°E and 23°E.

PA's signature on SST maps is much smaller; it is detected during wintertime only, but is almost not observed at all in 1993 and 1999. Using satellite-derived SST maps over the period 1983–1992, Marullo et al. (1999a) indicate as well that the Pelops gyre signature is observable from December to April only. The absence of an SST signal in summer when the presence of the anticyclone is evidenced on the SLA maps (Fig. 10) is not fully understood. On the one hand, we can assume that the basin-scale warming of surface waters in summer cancels the thermal contrast associated with the Pelops anticyclone. This would thus be an intrinsic problem to the use and interpretation of SST data in summer when the surface layers are (almost) uniformly heated. On the other hand, the reason may be physical, that is, linked to the vertical structure of the anticyclone itself. Indeed, as revealed by POEM data, the anticyclone has a deep vertical extension, with a temperature and salinity signature down to ~ 1650 m (Nittis et al., 1993). The associated dynamic height as computed by these authors shows a subsurface maximum. Moreover, as suggested by the maps of March–April and of September–October of Theocharis et al. (1993), the vertical structure is susceptible to change from one season to the other and from year to year. As a conclusion, we thus suggest that the Pelops anticyclone is a very stable structure of the Ionian basin circulation, in the sense that it is detected most of the time during the 7-year period of study. It displays a seasonal variability, consisting in a strengthening in fall–winter at the surface and in an area located south of the Peloponnese. In spring and, less commonly, in summer, it appears as a structure close to the western Greek coast

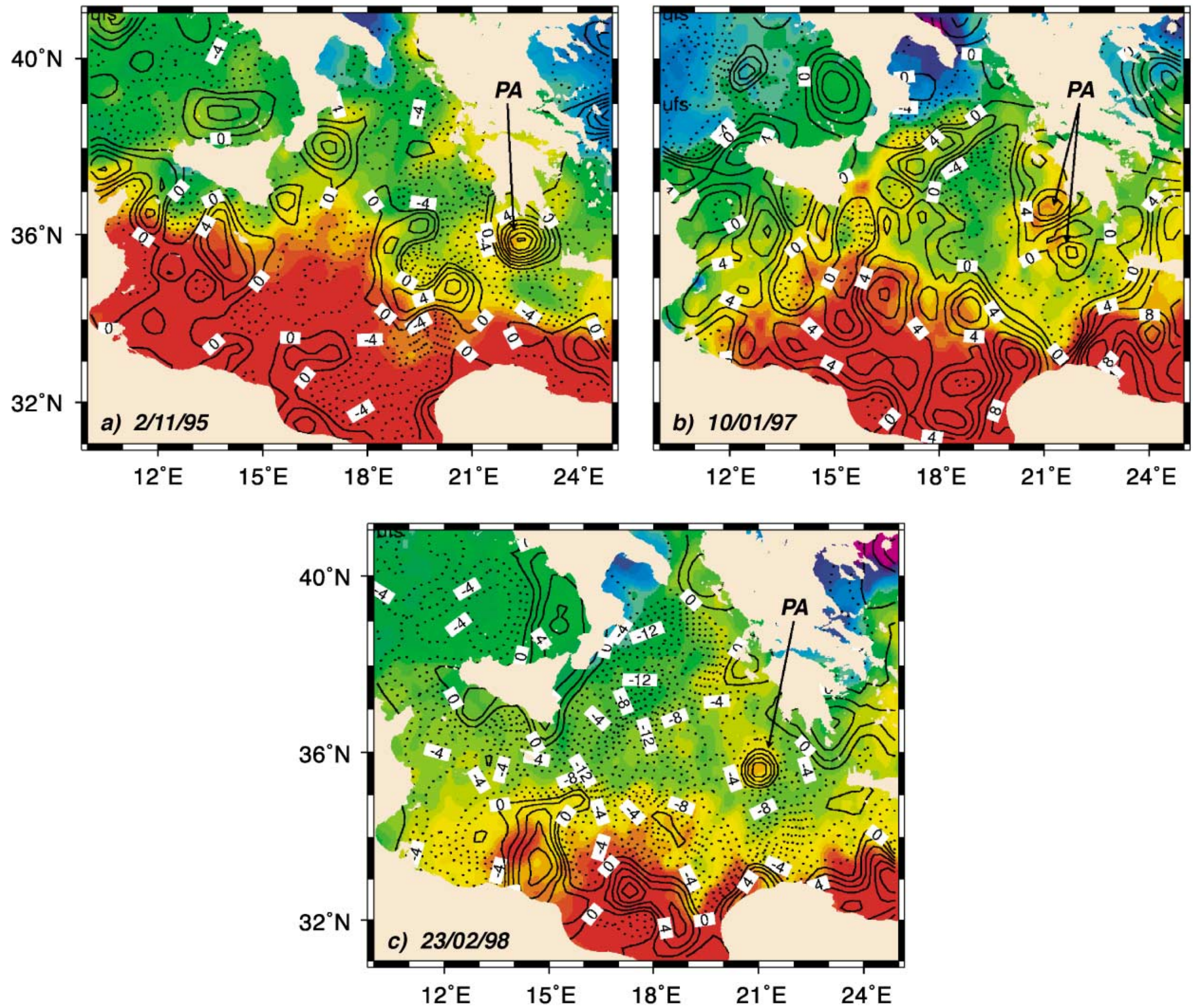


Fig. 12. Maps of SLA (contours spaced every 2 cm) and SST (colour) showing three different signatures of the Pelops anticyclone: (a) 2/11/95; (b) 10/01/97; (c) 23/02/98. N.B.: The SST scale is adapted for each figure to exhibit the most interesting gradient, so it is not indicated in the figure.

or southwest of it toward the center of the Ionian basin. In these latter situations, it is subsurface-intensified and does not exhibit any signature on the SST fields.

The mechanisms responsible for the generation and seasonal variability of PA are not yet understood. At the surface, one can assume that PA is affected by the basin-scale circulation and, in particular, by the IAS path (the summer path is expected to be parallel to the Peloponnese coast, see above). This would imply that PA seasonal cycle is influenced by wind stress variability. At depth, the Pelops anticyclone variability is probably more controlled by the circulation. Nittis et al. (1993) show that their water mass differs from the surrounding Ionian waters and have the characteristics of Aegean waters. We can thus assume that if water mass properties in the Cretan or Aegean seas are affected by interannual variability (such as the recent changes above mentioned), this would have a significant impact on the Pelops anticyclone signature in altimetric and SST data. This may explain the changes observed between 1993, 1999 and the period 1995–

Table 2
Occurrences of the Pelops anticyclone as seen on the 10-day maps of SST ('+') and of SLA ('O')

| | 1993 | 1994 | 1995 | 1996 | 1997 | 1998 | 1999 |
|---|---|---|---|---|---|---|---|
| January | O | O | + | + O | + O | + O | + O |
| | O | O | + | + O | + O | + O | O |
| | O | O | + | + | + O | + O | O |
| February | | + O | + | + | + | + O | O |
| | | + O | + | | + | + O | O |
| | | + O | | | + O | + O | O |
| March | O | + O | | | + O | + O | O |
| | O | O | + | | + | + O | O |
| | | O | + | | + O | + O | O |
| April | O | O | | | O | + O | O |
| | O | O | | | O | O | O |
| | O | O | | | O | O | O |
| May | O | O | | | | O | O |
| | O | O | | | | O | O |
| | O | O | | | | O | O |
| June | O | O | | | | O | O |
| | O | O | | | | O | O |
| | O | O | | | | | O |
| July | O | O | | | | | O |
| | O | O | | | | | O |
| | O | | | | | | O |
| August | O | | | | | | O |
| | O | | | | | O | O |
| | O | | | | | O | O |
| September | O | | | | | O | O |
| | O | | | | | O | O |
| | O | | | | | + O | O |
| October | O | | O | | O | + O | O |
| | O | O | O | | O | + O | O |
| | O | O | + O | + | O | + O | O |
| November | O | O | + O | + | O | O | O |
| | O | + O | + O | + O | O | + O | O |
| | O | + O | + O | + O | + O | + O | O |
| December | O | + O | + O | + O | + O | + O | + O |
| | O | + O | + O | + O | + O | + O | O |
| | + O | + O | O | + O | + O | + O | O |

The Pelops anticyclone is defined here as a single eddy or a multi-centered structure in the area roughly confined between 20–23°E and 35–37°N.

1998, but our study does not allow us to further explore this hypothesis.

## 6. Conclusion

We analyse the Mediterranean surface circulation variability using 7 years of combined altimetric data maps (1993–1999). This long period of observations and the merging of T/P and ERS altimeters data allow us to significantly improve the estimation of the variability given in previous studies (Larnicol et al., 1995; Iudicone et al., 1998; Ayoub et al., 1998). In particular, this new analysis evidences more complex structures than in the descriptions given previously. This is partly due to the complex combination of transient, seasonal and interannual signals. The latter makes it difficult to propose a stable scheme for the surface circulation variability, especially for the Levantine basin. Nevertheless, our long-term analysis reveals on the one hand the major seasonal and interannual signals during the 1993–1999 period, and on the other hand, the nature of Mediterranean Sea eddies in terms of transient, recurrent or permanent structures.

As a summary of the surface circulation variability over the years 1993–1999, we propose to distinguish two classes of structures. The first one concerns eddies that exhibit a stable position and a relatively structured temporal variability (e.g. seasonal), probably due to their forcing origin. These eddies are generally explicitly named. Conversely, the second class is associated to well-defined areas where eddies develop and are observed over periods varying from a few tens of days to several months. We interpret these structures as the signature of the mesoscale activity (eddies, meanders) of a current. This classification may appear somewhat artificial, but it allows us to confront our observations to previous studies based on in situ data (e.g. from POEM campaigns) or modeling.

We now summarize the main structures discussed in the paper; we list them in order of 'persistence nature'. The most intense and well-defined signals are the Western and Eastern Alboran gyres that exhibit a clear seasonal cycle with an intensification in summer. At seasonal scale, they are always present, except in 1999; this leads us to consider them as the most persistent gyres in the Mediterranean Sea. The Ierapetra eddy and the Pelops anticyclone are depicted on a less regular basis. However, they are usually observed over long periods and with consistent spatial structures between their different occurrences. Moreover, the Ierapetra eddy exhibits a strong seasonal signal. We consider them as recurrent features of the Mediterranean surface circulation. The Ierapetra eddy variability is assumed to be linked to the northern position of the MMJ and the direction and intensity of the Etesians winds. In the second type of structures, we include the well-known Algerian eddies that are associated with the Algerian Current instabilities. The analysis of the eddies situated in the Levantine basin, and especially in the Mersa-Matruh and Shikmona areas, shows that they do not appear at a fixed position and do not exhibit a clear temporal cycle. Our discussion is in agreement with the observational studies of Horton et al. (1994) and Matteoda and Glenn (1996) which conclude on the sporadic or recurrent occurrences of eddies rather than on the presence of permanent gyres. Furthermore, we suggest that these features are associated with the meanders of the MMJ.

A large interannual variability is evidenced in the Eastern basin. In the Ionian basin, drastic changes in the surface circulation have occurred since 1997, with a significant intensification of the cyclonic circulation in the north of the basin. This new situation is present until 1999. In the Levantine basin, the Ierapetra eddy undergoes large interannual variations. We can divide the 1993–1999 period into parts. The first one spans from 1993 to 1995 with the presence of a well-developed Ierapetra eddy that exhibits a seasonal cycle with a maximum in summer. During the second period (1995–1998), the Ierapetra eddy disappears, and is replaced by large anticyclones in the south. It seems that the situation in 1999 for the Ierapetra eddy is similar to the one in the 1993–1995 period. We suggest that the changes observed from 1995 in the Levantine and from 1997 in the Ionian are related to recent variations in the deep and intermediate water masses distributions in the whole Eastern basin. However, the respective role of the thermohaline circulation variations and of the local atmospheric forcing on the Ierapetra eddy variability and on the Ionian basin-scale circulation are still open questions.

## Acknowledgements

The work was funded by the MTP-II MATER under contract MAS3-EC CT96-0051 and by the MFSPP project (EU-MAST MA53-CT98 0171). Sea Surface Temperature products were produced by the CLS Space Oceanography Division as part of GANES (Global Assimilation applied to modelling of European Shelf Seas). CEO Contract: CT98-0744.

## References

Archiving, Validation and Interpretation of Satellite Oceanographic Data, 1996. AVISO Handbook for Merged TOPEX/POSEIDON Products, 3rd ed. Handb, AVI-NT-02-101-CN, Toulouse, France.

Ayoub, N., 1997. Variabilité du niveau de la mer et de la circulation en Méditerranée à partir de données altimétriques et de champs de vent; comparaison avec des simulations numériques. PhD Thesis, Univ. P. Sabatier, Toulouse, France.

Ayoub, N., Le Traon, P.Y., De Mey, P., 1998. A description of the Mediterranean surface circulation from combined ERS-1 and TOPEX/POSEIDON altimetric data. J. Mar. Syst. 18 (1–3), 3–40.

Beckers, J.M., Nihoul, J.C.J., 1992. Model of the Algerian current's instability. J. Mar. Syst., 441–451.

Brankart, J.-M., Brasseur, P., 1998. The general circulation in the Mediterranean Sea: a climatological approach. J. Mar. Syst. 18, 41–70.

Bretherton, F., Davis, R., Fandry, C., 1976. A technique for objective analysis and design of oceanographic experiments applied to MODE-73. Deep-Sea Res. 23, 559–582.

Centre ERS d'Archivage et de Traitement, 1996. Altimeter and Microwave Radiometer ERS Products User Manual. Handb. C2-MUT-A-01-IF, Brest, France.

Heburn, G., La Violette, P., 1990. Variations in the structure of the anticyclonic gyres found in the Alboran sea. J. Geophys. Res. 95, 1599–1613.

Horton, C., Kerling, J., Athey, G., Schmitz, J., Clifford, M., 1994. Airborne expendable bathythermograph surveys of the eastern Mediterranean. J. Geophys. Res. 99 (C5), 9891–9905.

Horton, C., Clifford, M., Schmitz, J., Kantha, L.H., 1997. A real-time oceanographic nowcast/forecast system for the Mediterranean Sea. J. Geophys. Res. 102, 25123–25156.

Iudicone, D., Santoleri, R., Marullo, S., Gerosa, P., 1998. Sea level variability and surface eddy statistics in the Mediterranean Sea from Topex/Poseidon data. J. Geophys. Res. 103 (C2), 2995–3011.

Klein, B., Roether, W., Manca, B.B., Bregant, D., Beitzel, V., Kovacevic, V., Luchetta, A., 1999. The large deep water transient in the Eastern Mediterranean. Deep-Sea Res., Part I 46, 371–414.

Larnicol, G., Le Traon, P.Y., Ayoub, N., De Mey, P., 1995. Mean sea level and variable surface circulation of the Mediterranean Sea from two years of TP altimetry. J. Geophys. Res. 100, 163–177.

La Violette, P., 1990. The Western Mediterranean Circulation Experiment (WMCE): introduction. J. Geophys. Res. 95 (C2), 1511–1514.

Le Traon, P.Y., Gauzelin, P., 1997. Response of the Mediterranean mean sea level to atmospheric pressure forcing. J. Geophys. Res. 102, 973–983.

Le Traon, P.Y., Ogor, F., 1998. ERS-1/2 orbit improvement using

TOPEX/POSEIDON: the 2 cm challenge. J. Geophys. Res. 103, 8045–8057.

Le Traon, P.Y., Nadal, F., Ducet, N., 1998. An improved mapping method of multi-satellite altimeter data. J. Atmos. Ocean Technol. 15, 522–534.

Malanotte-Rizzoli, P., Robinson, R., 1989. POEM, Physical Oceanography of the Eastern Mediterranean. Eos Trans. AGU 69, 4.

Marullo, S., Santoleri, R., Malanotte-Rizzoli, P., Bergamasco, A., 1999a. The sea surface temperature field in the Eastern Mediterranean from advanced very high resolution radiometer (AVHRR) data: Part I. Seasonal variability. J. Mar. Syst. 20, 63–81.

Marullo, S., Santoleri, R., Malanotte-Rizzoli, P., Bergamasco, A., 1999b. The sea surface temperature field in the Eastern Mediterranean from advanced very high resolution radiometer (AVHRR) data: Part II. Interannual variability. J. Mar. Syst. 20, 83–112.

Matteoda, A.M., Glenn, S.M., 1996. Observations of recurrent mesoscale eddies in the eastern Mediterranean. J. Geophys. Res. 101 (C9), 20687–20709.

Millot, C., 1985. Some features of the Algerian current. J. Geophys. Res. 90, 7169–7176.

Millot, C., 1999. Circulation in the western Mediterranean Sea. J. Mar. Syst. 20, 423–442.

Mortier, L., 1992. Les instabilités du courant Algérien. PhD, Univ. Aix-Marseille.

Nittis, K., Pinardi, N., Lascaratos, A., 1993. Characteristics of the summer 1987 flow field in the Ionian Sea. J. Geophys. Res. 98, 10171–10184.

Özsoy, E., Hetch, A., Ünlüata, U., Brenner, S., Sur, H.I., Bishop, J., Latif, M.A., Rozentraub, Z., Oguz, T., 1993. A synthesis of the Levantine basin circulation and hydrography, 1985–1990. Deep-Sea Res., Part II 40, 1075–1119.

Pascual, A., Buongiorno Nardelli, B., Larnicol, G., Emilianov, M., Gomis, D., 2002. A case of intense an anticyclonic eddy in the Balearic sea studied from satellite and in-situ data. J. Geophys. Res., in press.

Perkins, H., Kinder, T., La Violette, P., 1990. The Atlantic inflow in the western Alboran sea. J. Phys. Oceanogr. 20, 242–263.

Pinardi, N., Navarra, A., 1993. Baroclinic wind adjustment processes in the Mediterranean Sea. Deep-Sea Res., Part I 40, 1299–1326.

Puillat, I., Taupier-Lepage, I., Millot, C., 2002. Algerian eddies lifetimes can near 3 years. J. Mar. Syst. 31, 245–259.

Robinson, A.R., Golnaraghi, M., Leslie, W.G., Artegiani, A., Hetch, A., Lazzoni, E., Michelato, A., Sansone, E., Theocharis, A., Ünlüata, Ü., 1991. The Eastern Mediterranean general circulation: features, structure and variability. Dyn. Atmos. Oceans 15, 215–240.

Roether, W., Manca, B., Klein, B., Bregant, D., Georgopoulos, D., Beitzel, V., Kovacecic, V., Lucetta, A., 1996. Recent changes in the Eastern Mediterranean deep waters. Science 271, 333–335.

Roussenov, V., Stanev, E., Artale, V., Pinardi, N., 1995. A seasonal model of the Mediterranean Sea general circulation. J. Geophys. Res. 100, 13515–13538.

Speich, S., Madec, G., Crépon, M., 1996. A strait outflow circulation process study: the case of the Alboran sea. J. Phys. Oceanogr. 26, 320–340.

The MODB Group, 1996. Climatological atlas of the Mediterranean Sea. Scientific report of the last MAST-MODB initiative for ocean data and information management. Univ. of Liège, 253 pp.

Theocharis, A., Georgopoulos, D., Lascaratos, A., Nittis, K., 1993. Water masses and circulation in the central region of the eastern Mediterranean Ionian, South Aegean and northwest Levantine, 1986–1987. Deep-Sea Res., Part II 40, 1121–1142.

Theocharis, A., Nittis, K., Kontoyiannis, H., Papageorgiou, E., Balopoulos, E., 1999. Climatic changes in the Aegean Sea influence the Eastern Mediterranean thermohaline circulation (1986–97). Geophys. Res. Lett. 26, 1617–1620.

Tziperman, E., Malanotte-Rizzoli, P., 1991. The climatological seasonal circulation of the Mediterranean Sea. J. Mar. Res. 49, 411–434.

Vargas, M., Plaza, F., Garcia Lafuente, J., Vargas, J.M., Sarhan, T., 1999. The variability of the Alboran sea at different time and length scales. 4th Mediterranean Target Project Workshop, Perpignan, France, 28–30 October.

Vasquez-Cuervo, J., Font, J., Martinez-Benjamin, J.J., 1996. Observations on the circulation in the Alboran sea using ERS-1 altimetry and sea surface temperature data. J. Phys. Oceanogr. 26, 1426–1439.

Viudez, A., Tintore, J., Haney, R.L., 1996. Circulation in the Alboran sea as determined by quasi-synoptic hydrographic observations. Part I: Three-dimensional structure of the two anticyclone gyres. J. Phys. Oceanogr. 26, 684–705.

Zavatarelli, M., Mellor, G.L., 1995. A numerical study of the Mediterranean Sea circulation. J. Phys. Oceanogr. 25, 1384–1414.